INSTITUT DE FRANCE
Académie des sciences

Comptes Rendus

Physique

Philippe Bourges, Dalila Bounoua and Yvan Sidis

Loop currents in quantum matter

Volume 22, Special Issue S5 (2021), p. 7-31

Published online: 7 September 2021
Issue date: 11 May 2022

https://doi.org/10.5802/crphys.84

Part of Special Issue: Prizes of the French Academy of Sciences 2020

Les Comptes Rendus. Physique *sont membres du*
Centre Mersenne pour l'édition scientifique ouverte
www.centre-mersenne.org
e-ISSN : 1878-1535

Comptes Rendus
Physique
2021, 22, nº S5, p. 7-31
https://doi.org/10.5802/crphys.84

Prizes of the French Academy of Sciences 2020 / *Prix 2020 de l'Académie des sciences*

Loop currents in quantum matter

Philippe Bourges *, [a], **Dalila Bounoua** [a] **and Yvan Sidis** [a]

[a] Université Paris-Saclay, CNRS, CEA, Laboratoire Léon Brillouin, 91191, Gif-sur-Yvette, France

E-mails: philippe.bourges@cea.fr (P. Bourges), dalila.bounoua@cea.fr (D. Bounoua), yvan.sidis@cea.fr (Y. Sidis)

Prix CEA « science et innovation » de l'Académie des sciences 2020

Abstract. In many quantum materials, strong electron correlations lead to the emergence of new states of matter. In particular, the study in the last decades of the complex phase diagram of high temperature superconducting cuprates highlighted intra-unit-cell electronic instabilities breaking discrete Ising-like symmetries, while preserving the lattice translation invariance. Polarized neutron diffraction experiments have provided compelling evidences supporting a new form of intra-unit-cell magnetism, emerging concomitantly with the so-called pseudogap state of these materials. This observation is currently interpreted as the magnetic hallmark of an intra-unit-cell loop current order, breaking both parity and time-reversal symmetries. More generally, this magneto-electric state is likely to exist in a wider class of quantum materials beyond superconducting cuprates. For instance, it has been already observed in hole-doped Mott insulating iridates or in the spin liquid state of hole-doped 2-leg ladder cuprates.

Keywords. Loop-current, Quantum matter, Polarized neutron diffraction, High-temperature superconductors, Pseudo-gap, Magnetic correlations.

Available online 7th September 2021

1. Introduction

Strong electron correlations in condensed matter lead to the emergence of novel phenomena and exotic states. None of these collective phenomena is encompassed by the simple addition of individual electrons but results instead from many-body effects as it was advocated by Anderson almost 50 years ago [1]. Spin liquids, Mott physics, strange metals, high-temperature superconductivity and its related pseudogap phase are all typical examples of these novel states of matter, generically labeled as quantum matter.

The study of the complex phase diagram of hole-doped superconducting cuprates highlighted the existence of a mysterious state of matter, the so-called pseudogap (PG) metal [2–4], where large portions of the Fermi surface are gapped out and only Fermi arcs survive. The PG state is characterized by a significant loss of electronic entropy [5] below a certain temperature, so-called T^*, in the phase diagram, as represented in Figure 1. On cooling down, unconventional

* Corresponding author.

superconductivity with a d-wave symmetry occurs and seems to emerge out of the PG state. Furthermore, deep inside the PG state, an incipient charge density wave (CDW), with a d-wave structure factor, competes with superconductivity [2,3], while strong antiferromagnetic (AF) spin fluctuations are still present in the materials. The incipient CDW breaks the lattice translation (LT) symmetry and gives rise to a new periodicity associated with its modulation wave vector $\mathbf{q}_c \neq 0$. It coexists with a set of intra-unit-cell (IUC) electronic instabilities which preserve the LT invariance ($\mathbf{q} = 0$) (see e.g. [6–8]), but break discrete Ising-like symmetries: the fourfold rotation (R) symmetry for an electronic nematic state and additionally, time reversal (T) and parity (P) symmetries, as we shall discuss in details here. Remarkably, these different IUC orders show up concomitantly with the PG state. They are then necessarily tied up with it and should also be associated with a significant energy condensation. It should be stressed out that no additional noticeable change of the electronic entropy is reported below T^*, of course apart from the one associated with superconductivity [5]. This is, for instance, the case for states like the CDW occurring within the PG state. A central question is therefore which one of these order parameters is the primary one? It should be also stressed that there are two known mechanisms to open gaps in metals, either it results from a finite $\mathbf{q} \neq 0$ ordering breaking LT or it is due to a particle–particle pairing as does superconductivity. Therefore, none of the IUC broken symmetries alone can induce the needed fermionic gap characterizing the PG state.

To get a better understanding about these IUC orders, it is useful to look at the basic atomic structure of superconducting cuprates. They are layered perovskite materials, made of the stacking of CuO_2 layers, whose building block is a CuO_2 squared plaquette (Figure 3a–c). In the insulating undoped state, there is only a single electron on the Cu site carrying a half-integer spin $S = 1/2$. Upon hole doping, an extra hole on the O site can form a bound state with the electron on the Cu site, yielding the so-called Zhang–Rice singlet [9]. Owing to the strong on-site Coulomb repulsion which prevents a second hole to enter the plaquette, one is left with a set of three states for the CuO_2 squared plaquette, useful to build a minimum model (such as the widely studied $t-J$ model) for cuprates, but which also eliminate the internal degrees of freedom within the CuO_2 plaquette. In contrast, the IUC electronic orders imply the emergence of non-Zhang–Rice singlet states [10]. For an electronic nematic state, an unbalanced electronic density at the O sites breaks the fourfold R-symmetry of the CuO_2 plaquette, as observed in scanning tunneling microscopy (STM) [7,8].

Put altogether, the IUC symmetry breakings point towards novel electronic states that have been proposed either to account for or to characterize the PG state. That takes in particular the forms of loop currents (LCs) flowing coherently between copper and oxygen orbitals [4] as depicted in Figure 2a,b. LC states can take different shapes [23–28], where the electronic density remains uniform, but spontaneous charge currents appear between Cu and O sites within the CuO_2 plaquette. The circulating loop currents spontaneously break T-, P- and/or R-symmetries. The search for states of matter involving charge currents is a long story in the physics of high temperature superconductors and various states of matter were proposed. Unlike IUC and LC states (both being $\mathbf{q} = 0$ electronic instabilities), charge current density wave ($\mathbf{q} \neq 0$ electronic instability) were also proposed [29]. For instance, within a single band Hubbard model, charge currents were predicted to flow around the CuO_2 square lattice, yielding the so called "π-flux phase" or D-density wave (DDW) [30,31] which doubles the unit cell. As the π-flux phase breaks the LT symmetry, additional superstructure Bragg reflections are expected at several $\mathbf{Q}$-points in the reciprocal space equivalent to (π,π) [30,31]. Despite various attempts in different sets of samples, neutron diffraction measurements failed to prove the existence of magnetic peaks at the planar wave vector $(1/2,1/2) \equiv (\pi,\pi)$ in the 2D first Brillouin zone. As a generic property, all the types of charge current phases break T-symmetry and closed current loops generate a magnetic flux and orbital magnetic moments. That is the primary property reported to provide

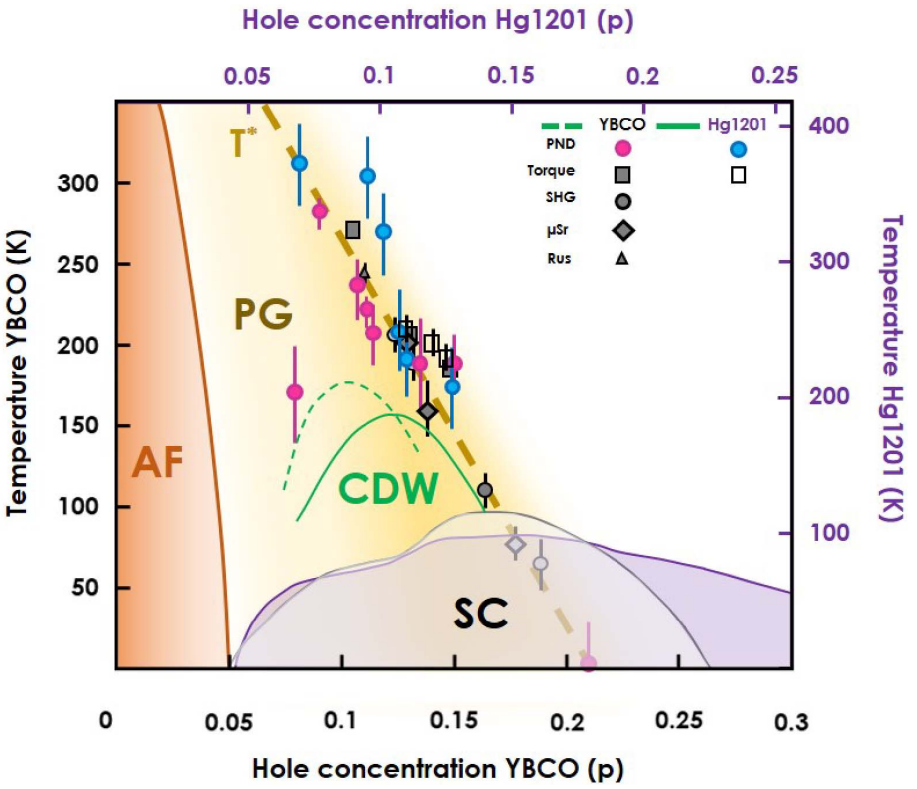

Figure 1. High-T_c superconducting cuprates phase diagram versus hole concentration for two cuprates families $YBa_2Cu_3O_{6+x}$ (YBCO) (bottom and right scales) and $HgBa_2CuO_{4+\delta}$ (Hg1201) (top and left scales) showing the intra-unit cell (IUC) magnetic order associated with the pseudogap state from polarized neutron diffraction (PND) [6, 11–17] and T^*, the pseudogap temperature, determined from torque [18, 19], second harmonic generation (SHG) [20], muon spectroscopy (μSR) [21] and resonant ultrasound (Rus) [22] experiments. Representative lines of transition of antiferromagnetism (AF), superconductivity (SC), pseudogap (PG) and charge density wave (CDW) (full line for YBCO and dashed line for Hg1201) are also depicted. The vertical and horizontal scales have been adapted to match T^* in both materials.

evidence in favor of the LC states in various quantum materials, and which experimentalists have tried to evidence by using dichroic effect using circularly polarized angle resolved photoemission (ARPES) [32] and next by looking for the LC induced orbital magnetism using polarized neutron diffraction (PND) as we shall review here in Section 2. To date, the LC state has been reported in several oxide materials either with 2D structure, in the superconducting cuprates [6,11–17,33–35] and in the iridates [36], or in the 1D spin ladder cuprate [37], showing the universal nature of this exotic state.

In this article, we next list in Section 3 the various experimental data (other than PND) that support the emergence of such LC states built from the LC-Θ_{II} pattern represented in Figure 2a. In particular, the macroscopic torque measurements in two cuprates families, namely in bilayer $YBa_2Cu_3O_{6+x}$ and monolayer $HgBa_2CuO_{4+\delta}$, [18, 19], although showing different results, match nicely the PND experiments [14, 15].

The remainder of the manuscript focuses in Section 4 on the interplay with the PG state, which

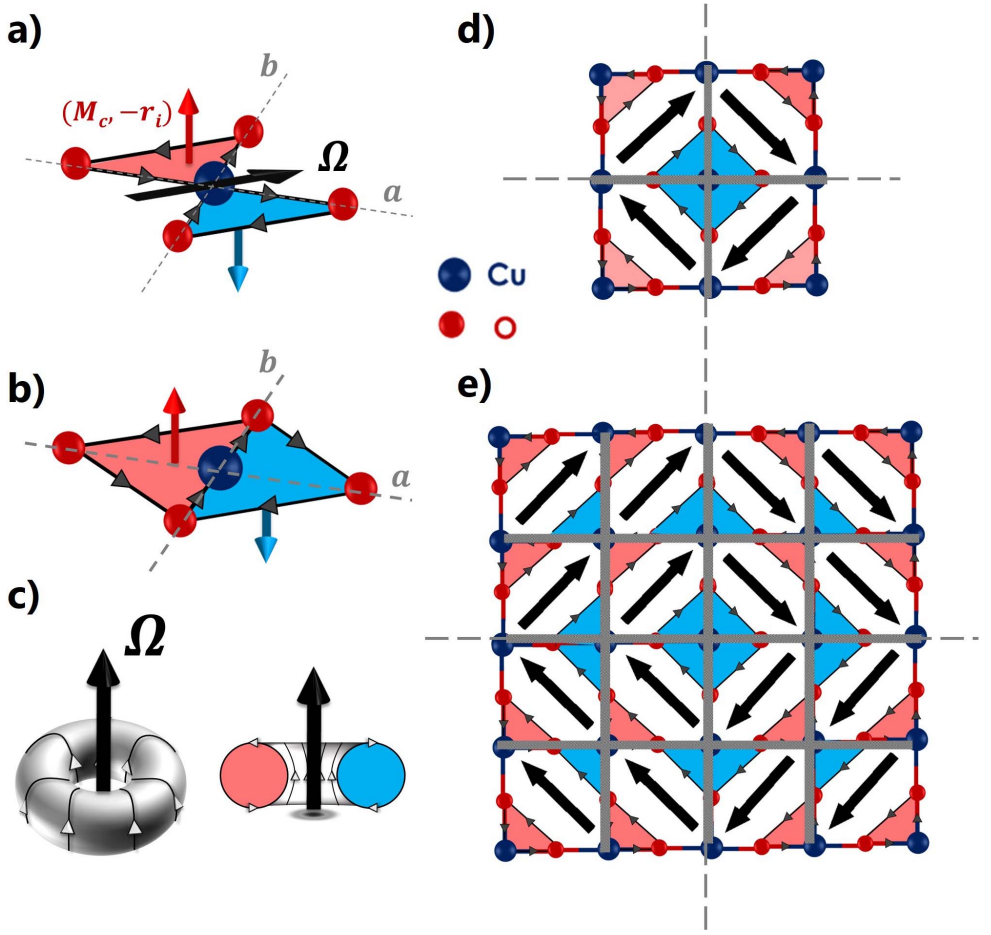

Figure 2. (a) Loop currents (LC) in CuO_2 plane, so-called LC-Θ_{II} phase, as proposed by Varma in superconducting cuprates [24, 25], with the corresponding toroidal moment, Ω, in black. (b) Model of loop currents proposed in Ref. [38]. The LCs now only run between oxygen sites, in contrast with the LC-Θ_{II} phase. (c) Anapole or polar toroidal moment Ω formed by winding current around a solenoid. A 2D section in the torus reveals two loop currents turning clockwise (blue) and anti-clockwise (red). (d) $(2P \times 2P)$ anapoles vortex crystal formed by LC-Θ_{II} supercells [28] obtained from a $\pi/2$ rotation of the anapole moment (in black) between neighbouring unit-cells. The magnetic cell encompasses the 4 possible domains for a LC pattern separated by domain walls (represented by the shaded lines). Here, the domains size as a function of the unit-cell is $P = 1$. (e) $(2P \times 2P)$ magnetic supercell for $P = 2$.

depends on the hierarchy among the various co-existing/competing observed phases. LCs can be bound to the PG physics in two ways. First, the LC phase is degenerate and several states corresponding to distinct LC patterns are allowed [25]. This degeneracy can be the source of a proliferation of randomly distributed LC domains. Assuming the existence of a super-cell made of a coherent juxtaposition of LC domains [28] (as shown by Figure 2d,e), the LT invariance would be broken and this modulated ($\mathbf{q} \neq 0$) LC-based phase could trigger a gap opening on the Fermi surface. Following a fundamentally different approach, the LC order can also be understood in

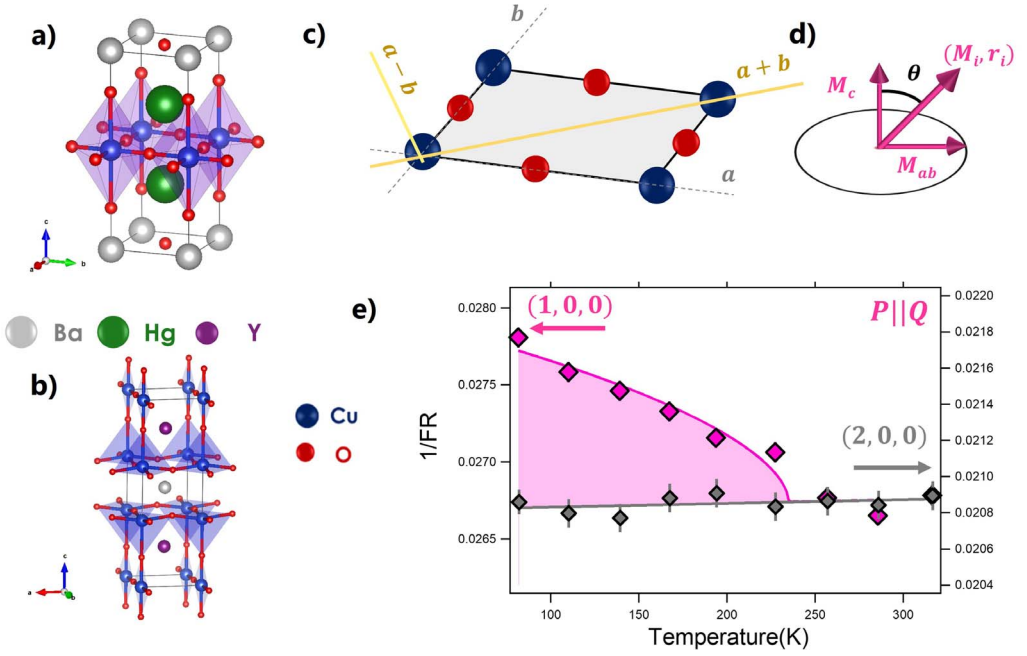

Figure 3. Crystal structure of layered perovskites (a) $HgBa_2CuO_{4+\delta}$ and (b) $YBa_2Cu_3O_{6+x}$. (c) CuO_2 plane with copper (blue circles) and oxygen (red circles) atoms. (d) Tilt of the observed magnetic moment. The magnetic moment is tilted by an angle θ from the c-axis direction, perpendicular to the CuO_2 plane. (e) Temperature dependencies of the inverse of the flipping ratio 1/FR (see text) measured at $\mathbf{Q} = (1,0,0)$ (purple) and at $\mathbf{Q} = (2,0,0)$ (gray), **P** is the neutron polarization parallel to **Q** to maximize the magnetic intensity (from [14]).

terms of a so-called "ancillary state" inseparable from the PG state [38–41]. The ancillary state is a secondary instability associated to a mother instability which itself effectively opens the PG. For instance, it can correspond to pair-density-wave (PDW) states [39–41]. Within these approaches, it was first pointed out by Agterberg *et al.* [39] that the LC phase necessarily happens owing to the symmetry and is therefore essential to capture the specific nature of the PG. We conclude in Section 5 with some perspectives for future experimental developments.

2. Polarized neutron diffraction experiments

Hunting for LCs, we have performed PND experiments on several correlated materials over the last 15 years. We here discuss layered perovskite materials with a (nearly) tetragonal structure within the **ab** basal plane corresponding to the (CuO_2 or IrO_2) layers (Figure 3c), stacked along the **c**-axis. The structural unit-cell contains one or more layers, depending on the materials, yielding different c lattice parameter. Examples of the corresponding crystallographic structure are shown in Figure 3a,b. The PND technique is a momentum-selective probe for magnetism. We commonly write, see e.g. Ref. [6], the measured momentum as $\mathbf{Q} = (H,K,L)$ in reduced lattice units $(2\pi/a, 2\pi/b, 2\pi/c)$ with $a \sim b \sim 3.85$ Å. Various attempts to observe the different orbital magnetic moments associated with the charge currents (π-flux or D-density wave) phase have been already discussed in [42,43].

2.1. *The IUC ($\boldsymbol{q} = 0$) magnetism*

Unlike the π-flux phase, the staggered orbital magnetism induced by the Varma's LCs [23–25] is associated with a set of pairs of charge currents looping clockwise and anticlockwise within each unit cell, Figure 2a [44]. Such a LC state preserves the LT symmetry, so that, in a diffraction experiment its magnetic Bragg reflections are superimposed to the structural Bragg reflections. This makes the experiments particularly difficult, as the magnetic contribution is weak, and polarized neutrons are required to discriminate between the structural and magnetic scatterings on a Bragg reflection. Indeed, any source of magnetism in the sample is able to flip the neutron spin, i.e. changing the spin polarization of the scattered neutron beam. To determine a possible orbital magnetic order, one needs to measure the variation of the neutron polarization versus temperature. A long range magnetic order would give rise to an upturn of the so-called inverse flipping ratio, 1/FR, which measures the ratio of magnetic to structural scatterings when the neutron polarization is set parallel to the scattering wavevector [6, 43]. A typical result is reported in Figure 3e where 1/FR ratio is shown versus temperature in the bilayer cuprate $YBa_2Cu_3O_{6.6}$ [14]. Two Bragg peaks are measured: at large $\mathbf{Q}$, (2,0,0), where the magnetic signal should vanish, an expected smooth thermal variation is reported whereas an upturn is observed around $T \simeq 235$ K at low $\mathbf{Q}$ = (1,0,0). This corresponds to the occurrence of a spontaneous magnetic signal. Assessment of the technical difficulties and limitations related to the PND experiments have been recently re-emphasized in [45].

Numerous PND measurements reveal the appearance of a $\mathbf{q} = 0$ antiferromagnetic order at the Bragg reflections $\mathbf{Q} = (1, 0, L)$ [43], also referred to as IUC magnetism [44]. This order displays a magnetic structure factor consistent with the orbital staggered magnetism produced by the LC-Θ_{II} state within the CuO_2 planes. In the field of unconventional high temperature superconductors, we reported such observations in four distinct cuprate families: $YBa_2Cu_3O_{6+x}$ [6, 11–14], $HgBa_2CuO_{4+\delta}$ [15–17], $(La,Sr)_2CuO_4$ [33], and $Bi_2Sr_2CaCu_2O_{8+\delta}$ [34, 35]. Figure 1 groups, in a generic phase diagram, the magnetic ordering temperatures measured by PND in the monolayer $HgBa_2CuO_{4+\delta}$ and bilayer $YBa_2Cu_3O_{6+x}$ compounds, as a function of the hole doping.

Later, we also reported an IUC magnetism in the large spin–orbit coupled Mott insulators, $Sr_2(Ir,Rh)O_4$ monolayer iridates [36], suggesting a more generic character of such LC orders in correlated electron oxides. It is worth noting that both iridates (Ir, 5d) and cuprates (Cu, 3d) are AF insulators which can be doped (Mott or charge-transfer insulators, respectively, and $S = 1/2$ on Cu versus $J = 1/2$ on Ir). Likewise, they share a similar layered perovskite structure. A noticeable difference with the 2D cuprates is that the LC occurs as well in the insulating compounds at half-filling, whereas in cuprates it is so far only observed in the doped metallic and superconducting materials, i.e. for a doping $\gtrsim$8% [12]. It is worth stressing out that the mechanism that could be invoked to produce LC state could differ in both oxides.

Despite the large body of PND data supporting an IUC magnetism in superconducting cuprates, its existence was questioned by a PND attempt [46], which failed to detect it in small $YBa_2Cu_3O_{6+x}$ single crystals (weighing less than 18 mg in contrast with our samples which weighted at least 2000 mg [47]). Due to the limited flux of polarized neutron beams and the relatively weak orbital magnetic moments, we demonstrated in [45, 47] that the experimental accuracy in [46] was clearly insufficient to draw any conclusions from the data as a consequence of the one well-known drawback of neutron scattering, which is the systematic need of large enough sample volume.

The PND results prove that the T-symmetry is broken when entering the PG phase of high-T_c superconducting cuprates, consistent with the LC-Θ_{II} phase symmetry (Figure 2a) originally proposed by Varma [24, 25]. The deduced spontaneous orbital magnetic moment is typically of the order of ~$0.1\mu_B$ per loop of the LC-Θ_{II} phase [43] and its magnitude decreases with increasing

hole doping following the trend of the pseudogap [6,35]. In general, it should be stressed out that PND data can be interpreted by a large number of magnetic models as long as these models produce compensated magnetic moments within a given unit cell and respect the LT symmetry. This is the case for instance for the Dirac multipole ordering proposed in Refs. [48–50], which we will discuss below. To conclude, a model accounting for the PND data needs at least two opposite magnetic moments in each unit cell, to comply with the $\mathbf{q} = 0$ antiferromagnetic structure.

2.2. *Magnetic moment direction*

The direction of the magnetic moments is experimentally determined through the neutron polarization analysis [43], from which one can deduce the magnitude of the out-of-plane component ($\mathbf{M}_c$) and the in-plane component ($\mathbf{M}_{ab}$). In the LC-Θ_{II} phase, the orbital magnetic moments should be perpendicular to the CuO_2 plane in which LCs are confined (Figure 2a,b). However, as sketched in Figure 3d, the outcome of the PND analysis is a $\Theta \sim 40 \pm 20°$ tilt angle of the magnetic moment with respect to the **c** axis. While systematically observed in all 2D cuprates [17], Θ can vary noticeably between the cuprates, as well as in function of the measured momentum **Q**-points. Interestingly, the moment tilt could also be temperature dependent [13]. Furthermore, as sketched in Figure 3d, the exact orientation of $\mathbf{M}_{ab}$ in the ab plane has not been determined experimentally yet. As a general remark, the observed tilt is not well accounted for by most of the theoretical models proposed for the IUC magnetism, as we shall see below. The observed tilt is certainly a key and unexpected feature of the observed IUC magnetism, putting stringent constraints on theoretical models.

2.3. *IUC spatial correlations*

Before, going further in the discussion, it is worth emphasizing some experimental limitations of the neutron scattering technique. Generally speaking, the neutron scattering cross-section is convoluted with the instrumental resolution of the instrument in 4 dimensions (**Q**, ω) [51]. The determination of the correlation length and characteristic time scale are limited by the instrument resolution. In order to detect a weak magnetic response, one usually relaxes the resolution. Likewise, a modulated structure, with a very long pitch, λ, gives rise to satellite reflections very close to the Bragg spot. These satellite scatterings can merge with the Bragg scattering owing to the experimental resolution. The canonical example is the long period helimagnet MnSi with $\lambda \sim 180$ Å, [52], for which the observation of the magnetic satellites requires the use of a very good resolution for diffraction measurements or the use of small angle neutron scattering techniques. In the latter case, the measurement is not performed around a Bragg reflection at finite $\mathbf{Q}$ ($\neq 0$) anymore, but around $\mathbf{Q} \rightarrow 0$. For LC-like magnetism, whose magnetic structure factor cancels for $\mathbf{Q} \rightarrow 0$, small angle neutron scattering is unfortunately unsuited.

In three of the cuprates families, namely $YBa_2Cu_3O_{6+x}$, $HgBa_2CuO_{4+\delta}$ and $Bi_2Sr_2CaCu_2O_{8+\delta}$, the observed IUC magnetism superimposes to the atomic Bragg peak [6, 15, 34, 43], suggesting that the IUC order is long range and 3D as it is clearly established in underdoped $YBa_2Cu_3O_{6.6}$ [11]. Due the relaxed instrument resolution that was used, only an upper limit of the correlation length along the c axis $\xi_c \leq 75$ Å could be given [11, 43]. As in MnSi, a situation with magnetic satellites with a long magnetic pitch could happen. Various attempts to observe a magnetic response in the reciprocal space distant from the Bragg position were however unsuccessful, giving a lower limit of a possible pitch of $\lambda \gtrsim 40$ Å. In an nearly optimally doped $YBa_2Cu_3O_{6.85}$ sample only, an IUC magnetic signal could be detected broader than the in-plane momentum resolution [13]. This indicates short range correlations with finite in-plane correlation lengths, $\xi_{ab} \sim 20a \sim 80$ Å in that compound.

A particularly interesting case is that of $La_{2-x}Sr_xCuO_4$, a system which is known to experience a segregation of doped holes into charge stripes [53]. For Sr substitution close to $x = 1/12$, we observed an IUC magnetic signal that remained quasi-2D with short range correlation lengths [33]. This contrasts with observations in other cuprates where a (quasi) long range IUC magnetism develops at 3D. This short range magnetism in lightly doped $La_{2-x}Sr_xCuO_4$ can be associated with very weak correlation lengths of LC-Θ_{II} 1D ribbons (~10 Å, i.e 2–3a). The short range magnetism can be viewed as LC-Θ_{II} objects confined on the charge stripes separated by hole poor AF domains of Cu spins, in relation with the charge order in this material [43, 53]. LCs can therefore interact with other electronic instabilities and persist in low dimensional systems (1D).

Following this observation and theoretical predictions [38, 54], we recently studied the 2-leg ladder cuprate $Sr_{14-x}Ca_xCu_{24}O_{41}$, which is an archetype of 1D spin liquids. This aperiodic system hosts a very rich phase diagram where, depending on the Ca content (which induces hole doping), it exhibits a strong spin liquid state ending into an intriguing ordered magnetic state at larger Ca content, passing through a CDW phase. Using PND, we discovered the existence of 2D short range magnetism in this material for two Ca contents [37]. This magnetism cannot be described by any type of Cu spins ordering. Instead, our investigations establish the existence of LC correlations within the 2-leg ladders [37]. The results from both studies suggest that LCs could be confined within quasi-1D structures, such as 2-leg Cu ladders, imposed either by the structure of the material in $Sr_{14-x}Ca_xCu_{24}O_{41}$ or by an electronic phase segregation yielding the formation of (bond centered-) stripes in $La_{2-x}Sr_xCuO_4$.

2.4. *L-dependence of the IUC magnetic structure factor*

The L dependence of the magnetic scattering associated with the IUC order has been reported for wavevectors $\mathbf{Q} = (1,0,L)$ in two monolayer compounds $HgBa_2CuO_{4+\delta}$ [15] and $La_{2-x}Sr_xCuO_4$ [33]. In the former, the magnetic signal from IUC order is only at integer L values, while it remains 2D (any L values) for the latter. Surprisingly, the scattered magnetic intensity displays the same fast decay as a function of L [34]. In principle, in bilayer compounds, in-phase or out-of-phase coupling between layers would give rise to a magnetic structure factor modulated either by a term $4\cos^2(\pi zL)$ or $4\sin^2(\pi zL)$, where $z(= d/c)$ stands for the reduced interlayer distance. Instead, the IUC magnetic pattern in $YBa_2Cu_3O_{6+x}$ exhibits a crisscrossed stacking of the IUC patterns [14] (as illustrated in Figure 5b), so that the L-dependence associated with the bilayer vanishes in the magnetic structure factor when dealing with a twinned crystal. Accordingly, the L-dependence of the scattered magnetic intensity measured in bilayer systems like twinned $YBa_2Cu_3O_{6+x}$ and $Bi_2Sr_2CaCu_2O_{8+\delta}$, matches that found for monolayer cuprates [34]. Furthermore, the calibration of the magnetic intensity measured on Bragg reflections with similar $|\mathbf{Q}|$ and in comparable samples, (i.e. at similar T^* and doping levels) indicates that the intensity for 2 Cu/f.u is only twice larger than the one measured for a single Cu/f.u, as if the (bi)layers were decoupled. Such a ratio is well acounted for by a crisscrossed arrangement of LCs within a bilayer [14].

The fast decay of the magnetic intensity along L observed in all cuprates is actually much faster than the one controlled by $|f(\mathbf{Q})|^2$ the squared magnetic form factor of Cu or O single ion [34]. This phenomenon could then be accounted for by IUC magnetic moments being spread out within the CuO_2 layer. In this picture, LCs would not be simply confined within the CuO_2 layers. They would be more delocalized than a magnetic moment bound to a single ion, giving rise to a faster decay of the IUC structure factor along the out-of-plane direction. This interpretation seems to be supported by the study carried out on twin-free samples: in this case, the scattered intensities along $(1,0,L)$ and $(0,1,L)$ differ and are weighted by $4\cos^2(\pi zL)$ and $4\sin^2(\pi zL)$,

respectively [14]. However, the observed ratio between the magnetic IUC intensities measured along a and b is not quantitatively reproduced with the reduced Cu–Cu distance, $z = 0.28$. A larger value of z provides a better result, suggesting that the magnetic moments could be located outside the CuO_2 layer. Such a property has not been observed yet in other materials exhibiting IUC order, such as iridates or 2-leg ladder cuprates.

3. Symmetry considerations

In both cuprates and iridates, PND shows the existence of an IUC magnetism, whose characteristic properties are consistent with the LC-Θ_{II} phase pattern breaking discrete T-, P- and four-fold R-symmetries. In addition to PND, complementary evidences of such broken symmetries were reported by other techniques, ranging from dichroism in circularly polarized ARPES spectroscopy [32], Kerr effect [55], Nernst effect [56], optical birefringence measurements [57], second harmonic generation (SHG) [20, 58], torque [18, 19, 59] and recently photo-galvanic effects [60], respectively. The Kerr effect was reported in cuprates and necessarily implies a global T-broken symmetry although this happens in $YBa_2Cu_3O_{6+x}$ [55] at a slightly lower temperature than the other experimental probes [6, 18, 20, 56, 57]. Each technique brings complementary information to draw the portrait of the IUC order and to guide theoretical models.

3.1. *Anapoles and quadrupoles*

The LC-Θ_{II} state is the ground reference of the observed IUC magnetic order. It is characterized by T- and P-symmetry breaking (although their product is preserved) [24, 25]. This view was reinforced in cuprates [58] and put forward in iridates [20] by the observation of P-symmetry breaking in SHG experiments at the same temperature as the T-symmetry breaking for a given doping. The LC-Θ_{II} magnetic pattern is described by two staggered orbital magnetic moments $\mathbf{M_i}$ located on a diagonal of the CuO_2 plaquette and equidistant from the Cu site. Within the basal lattice and for the state described in Figure 2a, the magnetic moments $\mathbf{M}_i = \pm(0, 0, \pm M_c)$ are then located at $\mathbf{r}_i = \pm(-r_0, r_0, 0)$. The LC-$\Theta_{II}$ exhibits, in principle, magneto-electric effects that can be described by a uniform arrangement of anapoles (also named: toroidal moments) [61]. The anapole Ω corresponds to a polar vector shown in Figure 2a constructed from the LC as,

$$\Omega = \sum_i \mathbf{r_i} \wedge \mathbf{M_i}. \tag{1}$$

In general, an anapole is described using a current flowing around a solenoid bent to form a torus (Figure 2c). The winding current around the solenoid generates a circular magnetic field inside the torus which gives rise to a pure anapole along the axis of the torus, according to the definition of Ω. In 2D, the 3D torus reduces to 2 LCs turning clockwise and anticlockwise. Actually, this staggered orbital magnetism supports not only an anapole, but also a magnetic quadrupole (3×3) tensor [62]. This is not surprising as the anapole appears at the same order of the magnetic multipole expansion as quadrupoles, as it is discussed in the context of multiferroics [62, 63]. More precisely, for the LC-Θ_{II} state, $\Omega = 2r_0M_c(\mathbf{a} + \mathbf{b})$ and the non-zero components of the magnetic quadrupole $Q_{ac} = Q_{bc} = r_0M_c$ [62].

LC-free models, involving Dirac multipoles, were actually developed to account for the IUC magnetic scattering reported by PND [48–50]. The CuO_2 plaquette is not occupied anymore by an anapole bound to LCs flowing through Cu and O, but by magnetic quadrupoles localized on the Cu site. Symmetry arguments are used to select the allowed magnetic quadrupoles, which can further ensure the P- and T-symmetries breaking [48–50]. Unlike electronic multiferroics where the charge and magnetic degrees of freedom form two distinct order parameters, these theoretical models predict the existence of new magneto-electric objects, in which the magnetic

and electronic degrees of freedom are intimately coupled to form a single exotic order parameter, for instance due to electron–phonon coupling [50].

Similarly to the magnetic distribution of the LC-Θ_{II} state, a magnetic distribution with only in-plane magnetic moments can be considered as well [62]: this corresponds to a pure magnetic quadrupole which is generated by a set of magnetic dipoles. Keeping the same notation as for the LC-Θ_{II} state, one could consider two magnetic moments $\mathbf{M}'_i = \pm(-M_{ab}, M_{ab}, 0)$, again located at $\mathbf{r}_i = \pm(-r_0, r_0, 0)$. The non-zero components of the magnetic quadrupole are $Q_{aa} = (1/3)Q_{ab} = -(1/2)Q_{cc} = (2/3)r_0 M_{ab}$ [62] and differ from the ones of the quadrupole above. These planar magnetic moments do not generate an anapole. The existence of such a magnetic quadrupole could then explain the observed in-plane component ($\mathbf{M}_{ab}$) of the IUC magnetism reported by PND, whereas the original LC-Θ_{II} state can only explain the measured out-of-plane component ($\mathbf{M}_c$). As one observes experimentally a tilted IUC moment, none of these magnetic distributions alone can describe the PND results. However, a combination of these two pictures could account for the tilted IUC moment as we shall see below (Section 3.3).

3.2. *Degeneracy of LC-Θ_{II} state*

It is worth emphasizing that the LC-Θ_{II} phase is characterized by four degenerate quantum states. The four LC patterns are deduced from each other by a 90° rotation with the anapole pointing along all diagonals of the basal plane [64, 65]. They produce four types of magnetic domains that will be summed up in bulk PND experiments (Figure 3e). If one considers a classical LC model, each of the LC domains gives a magnetic scattering in PND corresponding to magnetic moments perpendicular to the CuO_2 layer. In contrast, if a quantum superposition of the four LC states is allowed, then an effective planar magnetic response can appear as a result of quantum interference in the neutron scattering cross-section [65]. Therefore, the existence of the in-plane magnetic response could highlight the quantum effects in the LC state. The observation of a temperature dependent tilt angle in nearly optimally doped $YBa_2Cu_3O_{6.85}$ [13] could suggest a crossover from classical to quantum LC states, when thermal fluctuations are overcome by quantum ones. Within that scenario, quantum effects would then occur at relatively high temperature, around 200–250 K. This might be surprising unless the PG itself could impose the quantum superposition of the LC states which in turn produce the observed tilt [65].

3.3. *IUC point group symmetry*

Considering the simple crystal structure of a tetragonal monolayer system, such as $HgBa_2CuO_{4+\delta}$ (see Figure 3a), the LC-Θ_{II} state belongs to the magnetic point group $m'mm$ [25, 66] (m' is a mirror plane followed by a time reversal operation). The three mirror planes are respectively: the (**a+b**, **a-b**), (**a+b**, **c**) and (**a-b**, **c**) planes. Combining the above discussed magnetic distributions, one can build the magnetic pattern reported in Figure 4a with two magnetic moments $\mathbf{M}_i = \pm(M_{ab}, M_{ab}, M_c)$. This magnetic arrangement corresponds to a rotation of the LC-Θ_{II} magnetic pattern around the **(a-b)** diagonal axis, yielding a monoclinic magnetic point group $2/m'$ (as the rotation preserves the m' mirror plane) [66]. The magnetic pattern shown in Figure 4a differs from the one shown in Figure 4b where the planar magnetic component is aligned along the **(a-b)** axis (the moments are tipped out of the plane of the M_c components). The latter magnetic pattern has a magnetic point group $2'/m$ [66]. Note that the planar magnetic components of Figure 4b cannot be associated with a pure magnetic quadrupole only as in Figure 4a. Indeed, they give a contribution to an anapole ($-4r_0 M_{ab}\mathbf{c}$), in addition to the magnetic quadrupole ($Q_{aa} = -Q_{bb} = 2r_0 M_{ab}$). While being distinct, the magnetic patterns reported in Figure 4 produce hardly distinguishable neutron scattering cross-sections and fully account for the observed IUC

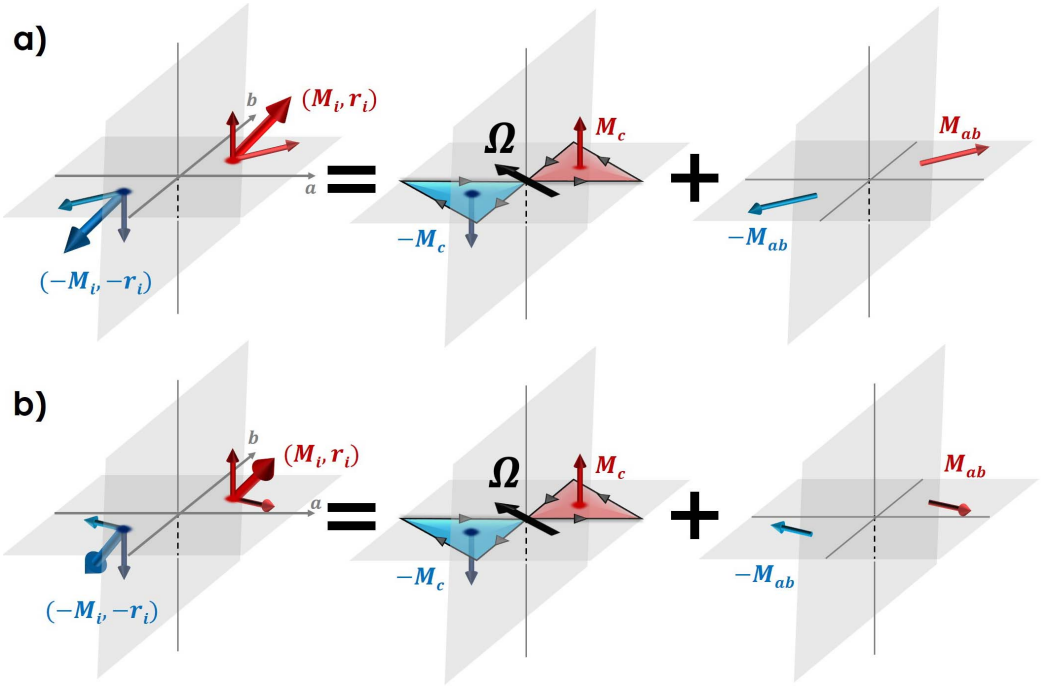

Figure 4. Representation of two possible magnetic moment arrangements which are compatible with the PND results. They correspond to a superposition of out-of-plane moments as the LC-Θ_{II} phase [24,25] with in-plane moments either (a) along the diagonal joining up the moments, or (b) along the perpendicular diagonal. This leads to different symmetries with (a) $2/m'$ point group and (b) $2'/m$ point group. Note that, as in Figure 2a, only one of the four possible LC states is shown.

magnetism. It should be stressed out that the $2'/m$ point group was deduced from SHG results in $YBa_2Cu_3O_{6+x}$ [58] based on (i) the observed $2/m$ symmetry of the atomic structure at 300 K and (ii) the broken global inversion related to the absence of C_2 axis.

In order to account for the existence of an in-plane magnetic component, one could also relax the constraint that LCs have to be confined within the CuO_2 plaquette. In hole doped cuprates, the Cu site is located at the center of an O octahedron in monolayer compounds, which splits in O pyramids in bilayer ones. The LCs could then be delocalized on the faces of the CuO_6 octahedra or on the CuO_5 pyramids, yielding a natural tilt of their orbital moments. However, the PND experiments exclude the LC states occurring on the faces of the CuO_6 octahedra [26, 66, 67] or on the CuO_5 pyramids [68] because the basal plane cannot also be a mirror plane for the in-plane component $\mathbf{M}_{ab}$. Only the LC state decorating the CuO_6 octahedra with only two opposite moments, as shown in Figure 5a and represented in [39, 67], is compatible so far with the PND results in $HgBa_2CuO_{4+\delta}$ [15–17] and belongs to the $2/m'$ point group. It should be stressed that no LC model on the CuO_5 pyramids has been found to be consistent with the PND data in bilayer materials.

Beyond the LC approach, a (Cu-)quadrupole modelling of the PND data [48–50] is also proposed with a magnetic structure belonging to $m'm'm'$ point group. It is actually not consistent with the data, as the basal plane cannot have a m' symmetry plane for the $\mathbf{M}_c$ component. This is due to the measurement of the magnetic structure factor at the $\mathbf{Q}$-position for $L = 0$ where a larger tilt is typically deduced [11, 17]. Other possible quadrupole arrangements [50] are then designed

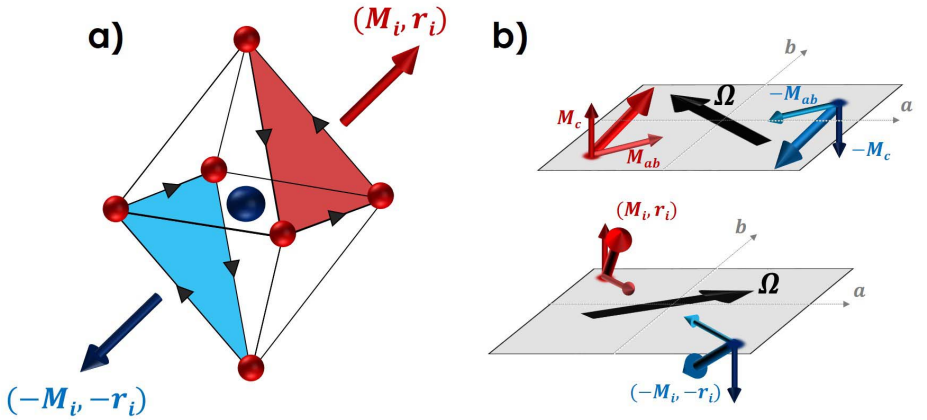

Figure 5. (a) Loop currents decorating a CuO_6 octahedron with two circulating loops [39, 67] which can describe the PND results in $HgBa_2CuO_{4+\delta}$ [15–17]. (b) Model of magnetic moments for a bilayer cuprate like $YBa_2Cu_3O_{6+x}$ built from the magnetic moment arrangement of a single layer shown in Figure 4a and compatible with the observed neutron structure factor [14].

to give a magnetic structure that belongs to the $2/m'$ point group.

In the bilayer $YBa_2Cu_3O_{6+x}$ system, the PND results in a twin-free sample [14] (see e.g. Figure 5b) are important as they rule out models [48, 50, 68], which assume either an in-phase or out-of-phase coupling of IUC order within a given bilayer. This dismisses models based on a magnetic nematic order, involving spin or orbital moments located at the O sites [6, 10] as well.

Linear and circular photo-galvanic effects recently observed at the PG temperature [60] in both monolayer and bilayer Bi-based cuprates suggest a $mm2$ point group symmetry, although monoclinic point group as $2/m'$ or $2'/m$ are also possible. A very interesting outcome of these experiments is the fact that the phase coherence of the IUC order should be as large as the size of the illuminated beam (~10 μm).

3.4. *Rotational symmetry breaking*

The different IUC phases proposed break R-symmetry. This can be tested in various experiments as, for instance, via the loss of both C_4 rotation and mirror symmetry in the electronic structure of the CuO_2 plane [57]. Indeed, the LC-Θ_{II} state imposes a preferential direction of the anapole along one of the diagonals of the CuO_2 plane. On the opposite, staggered LCs flowing on O sites only, as proposed in Refs. [38, 69], give a pattern rotated at 45° with respect to LC-Θ_{II} one and are characterized by an anapole along one of the CuO bonds (Figure 2b). However, owing to the formation of degenerate domains and assuming equal populations of the domains, PND cannot distinguish between these different magnetic models, see e.g. our results in 2-leg ladder cuprates [37]. Other techniques can provide information on the R-symmetry breaking. The broken fourfold R-symmetry is very often associated with the existence of electronic nematicity, which was reported using magnetic torque measurements in both cuprates [18, 19] and iridates [59]. In the monolayer $HgBa_2CuO_{4+\delta}$ compound, the torque magnetometry reports an anisotropy, $\chi_{ab} \neq 0$, along the diagonals of the CuO_2 plane [19], consistent with a distortion induced by the original LC-Θ_{II} state [61]. In monolayer iridates, torque experiments also show an electronic nematicity [59] with a nematic director, which is rotated by 45° from that of monolayer cuprate $HgBa_2CuO_{4+\delta}$. This implies different LC patterns between both systems, suggesting orbital-current configurations also turned by 45° (Figure 2b) [38, 69].

In the bilayer $YBa_2Cu_3O_{6+x}$ compound, there is a weak orthorhombicity ($a \neq b$) and an electronic nematicity was reported through Nernst effect measurements [56], showing the spontaneous appearance of a strong ab anisotropy. In addition, the torque magnetometry shows an anisotropy along the principal directions, with $\chi_{aa} > \chi_{bb}$ [18] i.e. turned by 45° from the single layer compound. Actually, the surprising difference in torque measurement results in monolayer $HgBa_2CuO_{4+\delta}$ and bilayer $YBa_2Cu_3O_{6+x}$ compounds can be solved by a close examination of the way LC-Θ_{II} patterns are stacked within a bilayer (along the **c**-axis) as shown by previous PND results [14]. Indeed, using a twin-free sample of the orthorhombic $YBa_2Cu_3O_{6.6}$, our PND results show a distinct ab anisotropy of the IUC magnetic structure factor [14], as a result of R-symmetry breaking. This highlights that the IUC order in this material breaks the mirror symmetry of the CuO_2 bilayer (Figure 5b). For a single CuO_2 plaquette, 4 LC patterns are allowed and, then, 4×4 LC patterns for a bilayer. Only 4 of them produce the magnetic structure factor matching the observed ab anisotropy found in PND measurements. They correspond to a crisscrossed arrangement of the LC patterns in the bilayer, yielding a resulting anapole, $\Omega_1 + \Omega_2$, parallel to **b** axis [14] as shown in Figure 5b. Note that each of the 4 selected LC patterns could be fully identified when using both their anapole and their chiral parameter, $\mathbf{c}(\Omega_1 \wedge \Omega_2)$.

From this result and using the corrugation of the CuO_2 plane (usually called dimpling in the literature), corresponding to the fact that Cu and O atoms lay in slightly different (but parallel) planes, one can construct a picture to explain the origin of the torque anisotropy (Figure 6a–d). Assuming that LCs run exactly within the Cu–O triangle, the dimpling of the CuO_2 layer induces a tilt of the out-of-plane moment, yielding a weak ferromagnetic in-plane component **M**, pointing perpendicular to the anapole Ω_i in each layer. As the total bilayer anapole is found to be along the **b** direction, the remaining weak ferromagnetic component for the bilayer is found also along **b** (Figure 6d). Accordingly, the magnetic torque τ, defined as $\tau \propto \mathbf{M} \wedge \mathbf{H}$ for an applied magnetic field **H** along **c**, is then expected to give an anisotropy along the **a** direction as it is reported in [18]. This simple picture gives a nice agreement between the microscopic picture deduced from PND experiment and the macroscopic torque measurements. It should be stressed that the weak ferromagnetic component would be averaged owing to the existence of the four domains of the LC-Θ_{II} state [64, 65].

Electronic nematicity was reported in the bilayer $Bi_2Sr_2CaCu_2O_{8+\delta}$ family as well, using either STM images of the IUC states [7,8,70,71] or electronic Raman scattering in the B_{1g} symmetry [72]. As in the bilayer $YBa_2Cu_3O_{6+x}$ material, a nematic director is found along the Cu–O bonds. Therefore, the nematic state in $Bi_2Sr_2CaCu_2O_{8+\delta}$ can be understood the same way assuming a similar crisscrossed arrangement of LCs within the CuO_2 bilayer, i.e. with a total anapole moment in the bilayer pointing along the Cu–O bonds. Alternatively, the LC-Θ_{II} state is a $\mathbf{q} = 0$ electronic state that could co-exist with other orthogonal $\mathbf{q} = 0$ electronic states, such as an electronic nematic state [73].

To conclude, the proposed LC-Θ_{II} represents the most adequate starting point to describe the IUC magnetism observed in PND experiments. It takes into account the various constraints imposed by symmetry even though additional features need to be considered.

4. Loop currents for cuprates

4.1. *Pseudogap line in cuprates: a phase transition*

Describing the generic experimental phase diagram shown in Figure 1, one realizes that the IUC order occurs at T^*, the PG onset temperature. The PG energy scale impacts a large number of experimental spectroscopic probes in cuprates, for instance electronic Raman scattering [74]. For a long time, the PG physics in 2D cuprates has been considered as a crossover phenomenon observed in various physical properties, occurring over a certain range of temperatures. No

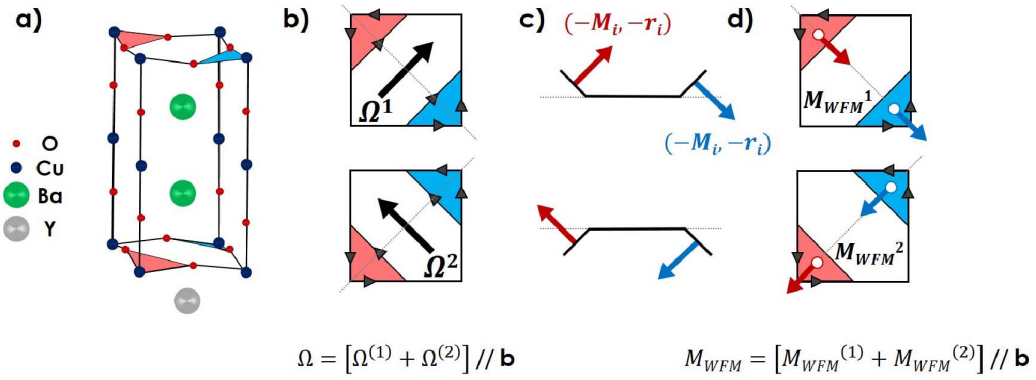

Figure 6. (a) Crystal structure of $YBa_2Cu_3O_{6+x}$, showing the corrugation or dimpling of the CuO_2 planes. (b) Top view of the loop currents arrangements of the LC-Θ_{II}-type in each CuO_2 layer (from [14]) where the toroidal moment is shown in black. The summed toroidal moment for a bilayer is pointing along the **b** direction. (c) Cut of the unit cell along the diagonal showing the orbital moments perpendicular to the O–Cu–O triangle. The dimpling of the O–Cu–O triangle gives rise to an horizontal magnetic component along the diagonal direction. (d) Top view of the summed magnetic moment, also pointing along **b**.

sharp anomaly was seen in the specific heat data, from which it was concluded that T^*, where the PG opens in transport measurements, cannot correspond to a thermodynamic phase transition [5]. In the recent years, as pointed out above, various symmetry breakings were identified over a much thinner range of temperatures. Independent measurements of an order parameter breaking T-, P- and R-symmetries agree on the location of a phase transition seen in experiments probing the thermodynamic properties. This is clearly established in three high-T_c superconducting cuprate families (the monolayer $HgBa_2CuO_{4+\delta}$, the bilayers $YBa_2Cu_3O_{6+x}$ and $Bi_2Sr_2CaCu_2O_{8+\delta}$). Figure 7 shows exclusively experimental results in $Bi_2Sr_2CaCu_2O_{8+\delta}$. That system is important to adress the issue of the PG because surface spectroscopic techniques can be performed as that material cleaves easily. Numerous ARPES [75] and tunneling spectroscopy of junctions [76, 77] studies have been performed to establish the depletion of the electronic states in that particular cuprate family. These estimates agree with T^* deduced from resistivity measurements [78] as well with those obtained from various spectroscopies [79, 80]. The IUC magnetism observed using PND was among the first reported order parameters in the PG state, which starts at a temperature T_{mag} that matches T^* (see Figures 1 and 7) and agrees with the downturn of the resistivity measurements in $YBa_2Cu_3O_{6+x}$ [6], in $HgBa_2CuO_{4+\delta}$ [15, 17] and in $Bi_2Sr_2CaCu_2O_{8+\delta}$ [78]. That suggested that the PG line corresponds to a true phase transition. Later, detailed analysis of the magnetization measurements [81], resonant ultrasound spectroscopy [22] and torque measurements [18, 19] demonstrated in both $YBa_2Cu_3O_{6+x}$ and $HgBa_2CuO_{4+\delta}$ that the PG line is truly a thermodynamic phase transition.

Although the reported features at T^* are rather weak in amplitude, they are all observed due to the higher accuracy of those techniques compared with specific heat data, where a large phonon background has to be removed. This establishes that the PG state is necessarily associated with an ordered state, a point that should be present in any model relevant for the physics of high-T_c cuprates. For instance, it is argued [82] that these results are compatible with the thermodynamics of the Ashkin–Teller model, which corresponds to the universality class of the LC-ordered phase, as this model does not produce any strong jump in the specific heat for a wide range of parameters [83].

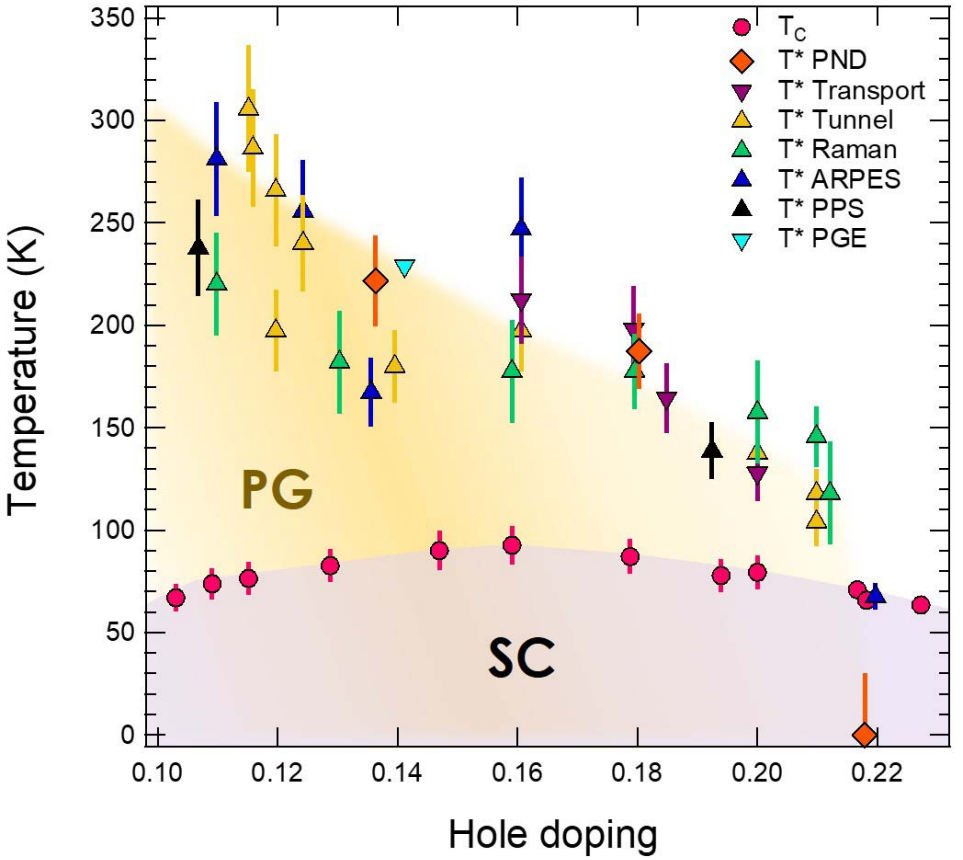

Figure 7. High-T_c superconducting cuprates phase diagram versus hole concentration for the cuprate family $Bi_2Sr_2CaCu_2O_{8+\delta}$ showing the intra-unit cell (IUC) magnetic order associated with the pseudogap state from polarized neutron diffraction (PND) [34, 35], transport [78], tunnel [76, 77], electronic Raman scattering [80], ARPES [75], pump probe spectroscopy (PPS) [79] and photo-galvanic (PGE) [60] experiments. Representative area for superconductivity (SC) and pseudogap (PG) are also depicted.

It has to be stressed that no other true symmetry-breaking phase than the IUC magnetism develops long range 3D correlation at T^*. Contrariwise, the incipient CDW phase develops at lower temperature (Figure 1), deep inside the PG state [2, 3] and remains short range and quasi-2D at zero magnetic field. That contrasts with the cases where uniform perturbations, such as a strong external magnetic field [84] or a uni-axial strain [85], are applied, which promote a long range ordered CDW, at the expense of superconductivity. If uniform perturbations can be used to tune the balance between superconductivity and CDW inside the PG state, the substitution by a minute amount of non magnetic (Zn) impurity on Cu site is sufficient to lower strongly the onset temperature of both states [86]. In contrast, the PG state [87] and the onset temperature of IUC magnetism [12] are both extremely robust against non magnetic impurity substitution. Furthermore, the IUC magnetism is reduced in amplitude through Zn substitution [12], in agreement with a picture established by NMR and STM [88] that the PG physics basically vanishes near Zn impurities, while remaining unchanged a few lattice spacings away from the impurity.

4.2. *Loop currents and pseudogap*

Because of its central play in the generic phase diagram, it is compulsory to consider PG physics in any scenario aiming at a description of the physics of cuprates. Being intimately tied to the PG state, the IUC magnetism, reported by PND, has to be implemented in any theoretical approach. Although the interplay between the LCs and the PG state is rather obvious from experimental results, its theoretical importance remains unclear as the proposed LC order in cuprates cannot open a PG at the Fermi level simply because it preserves LT symmetry [2]. Indeed, $\mathbf{q} = 0$ electronic instabilities in the electron–hole channel commonly split or distort the Fermi surface. This is the case for a ferromagnetic state, where two Fermi surfaces with different spin polarizations form in order to break the T-symmetry, or for an electronic nematic state where the Fermi Surface is distorted to break the R-symmetry. The only way to open a gap is then to break the LT-symmetry. Note, that superconductivity, which gaps the Fermi surface, is also a $\mathbf{q} = 0$ electronic instability, but in the electron–electron channel and it breaks a gauge symmetry. Therefore, one is left with two possibilities that we discuss below: (i) there is a hidden modulation of the IUC magnetism probed by PND, (ii) or the PG state is a distinct state of matter, intertwined with the IUC magnetism.

A modified version of the LC state, now breaking LT-symmetry, was recently proposed [28]. It consists of a LC super-cell of the four degenerate LC domains. Importantly, the next-nearest domain of a given domain should be characterized by an anapole rotated by $\pi/2$, either turned left or right, whereas the domain with an anapole rotated by π is only joining the first domain through its corners. The domains size, counted in number of unit cells P, ranges from a few cells to dozens of them. Examples of such phases are depicted in Figure 2d for $P = 1$ and in Figure 2e for $P = 2$. It is shown that domains of $P \sim$ 10–20 unit cells give rise to both a PG and Fermi arcs [28], as experimentally evidenced by ARPES and STM over the last two decades [2]. In this approach, the new magnetic unit cell is square, $(2P \times 2P)$ larger than the CuO_2 unit cell, and it is characterized by the planar wave vectors $\mathbf{q}_{\mathrm{LC}} = (1/2P, 0)$ and $(0, 1/2P)$. In a diffraction experiment like PND or resonant X-ray diffraction, this has major consequences, as the translation symmetry is now broken. Although this super-cell LC state has not been observed experimentally yet, it cannot be excluded from the current PND data sets if P is large enough. Indeed, in this case, the diffraction pattern has no maximum at the $(1, 0, L)$ or $(0, 1, L)$ Bragg reflections anymore, but gives rise to satellite reflections at $\pm\mathbf{q}_{\mathrm{LC}}$ away from them. If P were large enough, the diffracted peaks would occur as centered at the Bragg positions owing to the broad neutron instrument resolution, and to the limitations of the experiments with respect to the finite neutron polarization [43,45,47]. Furthermore, if there were a distribution of domains size P [89], it would lead to an effective broadening of the magnetic peaks appearing on the shoulders of the structural Bragg peaks.

The initial uniform LC phase can be as well considered as ancillary to a mother state associated with the PG state. For instance, square lattice spin liquid states are predicted to possess spontaneous LCs [38,69]. In the framework of a fractionalized spin density wave, the LCs also appear, forming an ancillary order, resulting from the intertwining between a topological order and the discrete Z_2 broken symmetries. In spin liquids, the emergence of LC orders in the archetype of doped 1D spin-liquids (hole-doped spin ladders) has been proposed [54]. Our recent results in spin-ladders [37] shows that local discrete symmetries are also broken in 1D spin liquid systems, as it has been theoretically predicted. In other models, based on a PDW state [39,40] or a fractionalized PDW instability [41], the PG is described as a highly fluctuating state, where a preemptive phase breaking both T- and P-symmetries (a LC-like phase) is expected at higher temperature. More generally, discrete symmetry breaking usually happens at higher temperature than continuous symmetry breaking. A strong influence of the LCs state on both unidirectional and bidirec-

tional d-wave charge-density-wave/pair-density-wave (CDW/PDW) composite orders has been emphasized [29, 90]. In these approaches, whatever the theoretical framework, the IUC LC order has to be intertwined with other states of matter [91]. For instance in Ref. [41], one starts with two primary states reported at lower temperature deep in the PG state (namely, the incipient CDW and superconductivity, both carrying a d-wave symmetry). The PG state is proposed to be a composite multi-component order parameter, where the system fluctuates between the two primary states which are intertwined. Then, the LC state would emerge as a preemptive state, born out of a higher order combination of the composite order parameters, which can be observed in the PG state (as soon as it forms), whenever the primary states still fluctuate or become static on cooling down.

Another interesting question is the relationship of the IUC magnetism with other $\mathbf{q} = 0$ electronic instabilities. In addition to the electronic nematicity observed through the Nernst effect in $YBa_2Cu_3O_{6+x}$ effect at T^* [56], enhanced electronic nematic fluctuations were observed close to the end point of the PG state at large hole doping [72]. However, they deviate from a canonical quantum critical scenario and cannot be directly associated with the PG state. Finally, the electronic nematicity could be inherited from another instability as suggested, for instance, by the sub-linear thermal dependence of torque measurements [18, 19]. This other instability could actually correspond to the LC state. Alternatively, it could be a vestigial order [92] related to the CDW, which exhibits a d-wave structure factor, implying that the electronic density on the O sites is involved [71]. At low temperature, the CDW breaks both the LT symmetry and the fourfold R-symmetry. At high temperature, when the CDW correlation length becomes shorter than the pitch of the modulation, the LT symmetry is restored and, the electronic nematic correlation only is left inside the unit cell. Both states can be viewed as the nematic (R-broken symmetry) and smectic (LT-broken symmetry) phases of an electronic liquid crystal. The role of IUC magnetism in this last approach remains unclear.

4.3. *IUC time-scale*

An important aspect of the IUC magnetic order seen in PND is that the local magnetic probes like nuclear magnetic resonance (NMR) and muon-spin rotation (μSR) are basically silent [43] because detecting the corresponding magnetic fields with magnetic resonance techniques has proved to be vastly unsuccessful, see e.g. in $HgBa_2CuO_{4+\delta}$ [93]. Another attempt using NMR in an ortho-II $YBa_2Cu_3O_{6+x}$ sample concluded that any static field at $T = 60$ K cannot be larger than ∼0.3 G at apical O site and ∼4 G at the planar O(2) sites [94]. For a static IUC magnetic order, a magnetic field of one order of magnitude larger is expected on these sites. The fact that the existence of a static long range IUC magnetism cannot be validated by NMR is a serious issue, which may question the outcome of the PND measurements. One possibility to reconcile NMR and PND data is to consider internal fluctuating fields at a timescale slow enough to appear static at the timescale of PND scattering (∼0.1 ns) but too fast to impact the NMR lines (≥10 μs).

The situation with μSR is more subtle. Since the first discovery of IUC magnetism with PND, it has been envisaged [6, 89, 95] that the magnetic moments could still fluctuate at the μSR timescale, meaning slowly enough to appear static to neutrons, but too fast to be observed as a magnetic order in μSR, therefore even more so for NMR, which probes even slower timescales. Several controversial results were reported by one team [95–97] but as a matter of fact, this interesting picture has been experimentally approved, as slow magnetic fluctuations were discovered using a longitudinal field μSR technique in $YBa_2Cu_3O_{6+x}$ compounds [21, 98] and in iridates [99].

In several $YBa_2Cu_3O_{6+x}$ underdoped samples [21, 98], at 80 K just above the superconducting temperature, the μSR measurements report magnetic correlations at a finite timescale of ∼10 ns

which fluctuate slowly enough to give rise to resolution-limited magnetic peaks in a PND experiment. Furthermore, this time-scale does not appear to be strongly temperature dependent. Such a finite time-scale associated with finite spatial domains was proposed to happen if defects limit the magnetic correlation length [89]. Short range correlations with finite in-plane correlation lengths, $\xi \sim 20a$, were actually detected in nearly optimally doped $YBa_2Cu_3O_{6+x}$ using PND [13]. As discussed above, shorter in-plane IUC correlation lengths are even observed in other cuprates, limited either by the competition with charge stripes in $(La,Sr)_2CuO_4$ [33] or by dimension in two-leg spin ladder compounds [37]. Clearly, dimension, disorder and proliferation of magnetic domains associated with degenerate LC states all can play a role.

The magnetic correlations seen by μSR can therefore be associated with slowly fluctuating magnetic domains. Interestingly, these fluctuations are maximum at the same temperature $T_{\rm mag} \sim T^*$ at which the neutron magnetic signal sets in [21, 98]. This suggests a critical slowing down of these magnetic fluctuations at T^*, associated with the PG onset. Such dynamical fluctuations at T^* have also been detected by PND in nearly optimally doped $YBa_2Cu_3O_{6+x}$ [13] and in $HgBa_2CuO_{4+\delta}$ at two hole doping levels [17].

4.4. *Possible roles of loop currents*

As it does not affect the LT symmetry, the original LC states are usually not considered as a key player for the physics of high-T_c superconducting cuprates. It is typically much less discussed than CDW, stripes physics or AF fluctuations [2, 3]. This might be for two main reasons. First, it is a more exotic phenomenon with, so far, a limited number of realizations in nature. The recent observation of P- [20], T- [36] and R- [59] symmetry breaking in $(Sr,Rh)_2IrO_4$ iridates clearly opens new frontiers as it basically corresponds to a LCs picture [25, 69]. Second, it is a state which involves not only copper orbitals but also oxygen orbitals. This orbitals mixing with an electronic phase gradiant among the three d and p orbitals is a central feature, which imposes a three-band Hubbard model as a starting point [25, 27, 38]. A large majority of the models built for cuprates usually neglects the possible role of oxygen orbitals, as the band structure is nicely reproduced by a single renormalized band electronic structure observed in ARPES and STM [2].

Numerical calculations using different methods still give contrasted pictures, even for three-band Hubbard model. On the one hand, variational Monte Carlo calculations on asymptotically large lattices and exact diagonalization on a 24-site cluster show a stabilization of the LC-Θ_{II} for a wide range of parameters [27]. On the other hand, no instance of spontaneous LCs has been found by applying cluster dynamical mean field theory in ladder cuprates [100] in materials where they have been observed [37]. As a matter of fact, variational Monte Carlo is a method to determine ground states at zero temperature, in contrast to the dynamical mean field theory, which is typically more efficient at finite temperature.

Generally speaking, LCs could be of great fundamental interest for several reasons. First, their fluctuations could be involved in the pairing mechanism and thus explain high-temperature superconductivity [64]. Within that scenario, the electrons are paired through the coupling of their local angular momentum to an operator defined as the generator of the rotations in the space of the four degenerate states discussed above. The corresponding pairing vertex favors d-wave superconductivity and is also proportional to the LC order susceptibility. Along similar lines, a novel spin-fluctuation-driven charge loop current mechanism based on the functional renormalization group theory has been proposed [101]. The discussed mechanism leads to ferro-LC order in a simple frustrated chain Hubbard model, which indicates that the LC can be universal in strongly correlated electron metals near magnetic criticality with geometrical frustration.

In the normal state, the related density susceptibility takes the functional form hypothesized for the Marginal Fermi liquid or strange metals [4]. Namely, it should be rather independent of momentum and with almost structure-less energy dependence. Such a charge response has been recently measured in cuprates using a new technique probing the charge-charge correlation function [102]. It is argued that it corresponds to the density susceptibility expected for the LC fluctuations in the normal state [4]. Interestingly, LC states are thought to be an emergent phenomenon, important for the establishment of the strange metals physics [103]. More specifically, if a scaling ω/T of the low energy dependence of the conductivity is observed, it must be due to the fluctuations of an order parameter which is a vector that breaks T and P symmetries and has zero crystal momentum [103]. That is a precisely the statement for LC order.

LC orders could also be of particular importance in certain theories of the PG state in cuprates in relation with topological orders [38] or emanating from the fluctuations of a vectorial order parameter [41, 104] as discussed above.

5. Conclusions and perspectives

In this brief overview, arguments were listed in favor of the physics of LCs in quantum materials. Numerous experiments that include PND point towards the existence of an exotic LC order parameter that does not break the LT symmetry. At a microscopic level, this corresponds to an electronic state phasing d orbitals of the transition metals with the ligand p orbitals. To some extent, the observed phenomenon could also be described by the ordering of magnetic quadrupoles of the transition metals [48, 50]. All these order parameters, anapoles, quadrupoles or orbital currents curls have in common the breaking of both T- and P-symmetries and the conservation of their product. These objects have dual (magnetic and electric) character order parameter, leading to interesting new applications for magneto-electricity [105]. For instance, they are proposed for potential applications in the field of data storage, where it would be possible to control magnetization via the application of an electric field, and thus use these toroidal domains as magnetic qubit [63].

In this context, future developments will aim at exploring and generalizing the observation of these new exotic objects in a wider range of materials. That will follow several directions: for instance, the Fe-based superconducting materials could host as well such a phase. It is actually proposed that the spin–orbit coupling present in the pnictides enforces the emergence of orbital loop current order inside the usual stripe-type spin-density wave state [106]. In any case, the investigation of LCs in other families of cuprate compounds using PND, namely in CuO, $Sr_2CuO_2Cl_2$ and $La_{2-x}Ba_xCuO_4$ should be pursued. In CuO, LCs were reported by a resonant X-ray scattering study [107], though this interpretation is not necessarily supported by later experiments and simulations [62, 108]. In $Sr_2CuO_2Cl_2$, a recent optical SHG experiment points towards a magneto-chiral state [109]. Following previous PND results [33], studying $La_{2-x}Ba_xCuO_4$ will allow one to probe the competition between the IUC magnetic order and other electronic instabilities, in that particular case the long range ordering of charge stripes [110]. All these examples should address the important question of the coexistence of LC phases with AF order in highly hole doped cuprates.

Another route to explore the magnetism related to the anapoles or quadrupoles is to use resonant X-ray diffraction at the appropriate atomic edge [49, 62, 107, 108]. Unlike usual non-resonant X-ray diffraction, the magnetic signal is enhanced at the resonant energy threshold of atomic electronic transitions. This technique, sensitive to both T- and P-symmetries, allows the separation of the magnetic signal from the atomic signal, by the use of linear or circular polarization analysis of the scattered beam. It allows one to selectively probe dipole, quadrupole transitions or the interaction between these two processes. A key advantage is the ability to select

the ion whose electronic transitions are induced by proper selection of the incident X-ray energy. For cuprates, measurements need to be carried at the absorption K-edge of Cu in order to access the terms corresponding to the anapoles, as derived from the multipolar expansion series. The IUC magnetic ordering observed in PND should induce an additional contribution to the anomal structure factor. For example, at the Cu K-edge (8985 eV), a dipolar–quadrupolar interference term (E1-E2) should occur with a characteristic dependence as a function of the azimuthal angle. This experiment certainly represents an important challenge.

Finally, the LC story has not been completed yet. The exact interplay between LC states and high-T_c superconductivity needs more experimental results, which will contribute to consolidate the theoretical models and to complete them. We hope our discovery will open up a new field of study when addressing the physical properties of highly correlated electron materials.

Glossary

AF	Antiferromagnetic/antiferromagnetism
ARPES	Angle resolved photoemission
CDW	Charge density wave
IUC	Intra-unit-cell
LC	Loop current
LT	Lattice translation
μSR	Muon spectroscopy/muon-spin rotation
NMR	Nuclear magnetic resonance
P	Parity
PDW	Pair density wave
PG	Pseudogap
PND	Polarized neutron scattering
R	Rotational
SHG	Second harmonic generation
STM	Scanning tunneling microscopy
T	Time

Acknowledgements

The authors are deeply indebted to C. M. Varma who first proposed to search for a loop currents phase in high-T_c cuprates and has been suggesting appealing novel ideas ever since. We acknowledge also the many students and colleagues who contributed to this work either in France, V. Balédent, S. de Almeida, B. Fauqué, Jaehong Jeong, L. Mangin-Thro, S. Pailhès or within our international collaborations, M. Greven, Yuan Li and all our collaborators whose names appear in Refs. [6, 11–17, 33–37]. We wish to thank F. Damay, A. Georges, T. Giamarchi, S. Lovesey, C. Pépin, E. Tailleur, A. Shekhter and J. Villain for stimulating discussions on various aspects related to this work. We acknowledge financial supports from the project NirvAna (Contract ANR-14-OHRI-0010) of the Agence National de la Recherche (ANR) French agency.

References

[1] P. W. Anderson, "More is different", *Science* **177** (1972), p. 393-396.

[2] B. Keimer, S. A. Kivelson, M. R. Norman, S. Uchida, J. Zaanen, "From quantum matter to high-temperature superconductivity in copper oxides", *Nature* **518** (2015), p. 179-186.

[3] C. Proust, L. Taillefer, "The remarkable underlying ground states of cuprate superconductors", *Annu. Rev. Condens. Matter Phys.* **10** (2019), no. 1, p. 409-429.

[4] C. M. Varma, "Colloquium: linear in temperature resistivity and associated mysteries including high temperature superconductivity", *Rev. Mod. Phys.* **92** (2020), article no. 031001.

[5] J. Loram, J. Luo, J. Cooper, W. Liang, J. Tallon, "Evidence on the pseudogap and condensate from the electronic specific heat", *J. Phys. Chem. Solids* **62** (2001), no. 1, p. 59-64.

[6] B. Fauqué, Y. Sidis, V. Hinkov, S. Pailhès, C. T. Lin, X. Chaud, P. Bourges, "Magnetic order in the pseudogap phase of high-T_C superconductors", *Phys. Rev. Lett.* **96** (2006), article no. 197001.

[7] K. Fujita, C. K. Kim, I. Lee, J. Lee, M. H. Hamidian, I. A. Firmo, S. Mukhopadhyay, H. Eisaki, S. Uchida, M. J. Lawler, E.-A. Kim, J. C. Davis, "Simultaneous transitions in cuprate momentum-space topology and electronic symmetry breaking", *Science* **344** (2014), no. 6184, p. 612-616.

[8] K. Fujita, M. H. Hamidian, S. D. Edkins, C. K. Kim, Y. Kohsaka, M. Azuma, M. Takano, H. Takagi, H. Eisaki, S.-i. Uchida, A. Allais, M. J. Lawler, E.-A. Kim, S. Sachdev, J. C. S. Davis, "Direct phase-sensitive identification of a d-form factor density wave in underdoped cuprates", *Proc. Natl Acad. Sci. USA* **111** (2014), no. 30, p. E3026-E3032.

[9] F. C. Zhang, T. M. Rice, "Effective Hamiltonian for the superconducting Cu oxides", *Phys. Rev. B* **37** (1988), p. 3759-3761.

[10] A. S. Moskvin, "Pseudogap phase in cuprates: oxygen orbital moments instead of circulating currents", *JETP Lett.* **96** (2012), p. 385-390.

[11] H. A. Mook, Y. Sidis, B. Fauqué, V. Balédent, P. Bourges, "Observation of magnetic order in a superconducting $YBa_2Cu_3O_{6.6}$ single crystal using polarized neutron scattering", *Phys. Rev. B* **78** (2008), article no. 020506.

[12] V. Balédent, D. Haug, Y. Sidis, V. Hinkov, C. T. Lin, P. Bourges, "Evidence for competing magnetic instabilities in underdoped $YBa_2Cu_3O_{6+x}$", *Phys. Rev. B* **83** (2011), article no. 104504.

[13] L. Mangin-Thro, Y. Sidis, A. Wildes, P. Bourges, "Intra-unit-cell magnetic correlations near optimal doping in $YBa_2Cu_3O_{6.85}$", *Nat. Commun.* **6** (2015), article no. 7705.

[14] L. Mangin-Thro, Y. Li, Y. Sidis, P. Bourges, "$a-b$ anisotropy of the intra-unit-cell magnetic order in $YBa_2Cu_3O_{6.6}$", *Phys. Rev. Lett.* **118** (2017), article no. 097003.

[15] Y. Li, V. Balédent, N. Barisic, Y. Cho, B. Fauqué, Y. Sidis, G. Yu, X. Zhao, P. Bourges, M. Greven, "Unusual magnetic order in the pseudogap region of the superconductor $HgBa_2CuO_{4+\delta}$", *Nature* **455** (2008), no. 7211, p. 372-375.

[16] Y. Li, V. Balédent, N. Barišić, Y. C. Cho, Y. Sidis, G. Yu, X. Zhao, P. Bourges, M. Greven, "Magnetic order in the pseudogap phase of $HgBa_2CuO_{4+\delta}$ studied by spin-polarized neutron diffraction", *Phys. Rev. B* **84** (2011), article no. 224508.

[17] Y. Tang, L. Mangin-Thro, A. Wildes, M. K. Chan, C. J. Dorow, J. Jeong, Y. Sidis, M. Greven, P. Bourges, "Orientation of the intra-unit-cell magnetic moment in the high-T_c superconductor $HgBa_2CuO_{4+\delta}$", *Phys. Rev. B* **98** (2018), article no. 214418.

[18] Y. Sato, S. Kasahara, H. Murayama, Y. Kasahara, E.-G. Moon, T. Nishizaki, T. Loew, J. Porras, B. Keimer, T. Shibauchi, Y. Matsuda, "Thermodynamic evidence for a nematic phase transition at the onset of the pseudogap in $YBa_2Cu_3O_y$", *Nat. Phys.* **13** (2017), p. 1074-1078.

[19] H. Murayama, Y. Sato, R. Kurihara, S. Kasahara, Y. Mizukami, Y. Kasahara, H. Uchiyama, A. Yamamoto, E.-G. Moon, J. Cai, J. Freyermuth, M. Greven, T. Shibauchi, Y. Matsuda, "Diagonal nematicity in the pseudogap phase of $HgBa_2CuO_{4+\delta}$", *Nat. Commun.* **10** (2019), article no. 3282.

[20] L. Zhao, D. H. Torchinsky, H. Chu, V. Ivanov, R. Lifshitz, R. Flint, T. Qi, G. Cao, D. Hsieh, "Evidence of an odd-parity hidden order in a spin–orbit coupled correlated iridate", *Nat. Phys.* **12** (2016), p. 32-36.

[21] J. Zhang, Z. Ding, C. Tan, K. Huang, O. O. Bernal, P.-C. Ho, G. D. Morris, A. D. Hillier, P. K. Biswas, S. P. Cottrell, H. Xiang, X. Yao, D. E. MacLaughlin, L. Shu, "Discovery of slow magnetic fluctuations and critical slowing down in the pseudogap phase of $YBa_2Cu_3O_y$", *Sci. Adv.* **4** (2018), no. 1, article no. eaao5235.

[22] A. Shekhter, B. J. Ramshaw, R. Liang, W. N. Hardy, D. A. Bonn, F. F. Balakirev, R. D. McDonald, J. B. Betts, S. C. Riggs, A. Migliori, "Bounding the pseudogap with a line of phase transitions in $YBa_2Cu_3O_{6+x}$", *Nature* **498** (2013), p. 75-77.

[23] C. M. Varma, "Non-Fermi-liquid states and pairing instability of a general model of copper oxide metals", *Phys. Rev. B* **55** (1997), p. 14554-14580.

[24] M. E. Simon, C. M. Varma, "Detection and implications of a time-reversal breaking state in underdoped cuprates", *Phys. Rev. Lett.* **89** (2002), article no. 247003.

[25] C. M. Varma, "Theory of the pseudogap state of the cuprates", *Phys. Rev. B* **73** (2006), article no. 155113.

[26] C. Weber, A. Läuchli, F. Mila, T. Giamarchi, "Orbital currents in extended hubbard models of high-T_c cuprate superconductors", *Phys. Rev. Lett.* **102** (2009), article no. 017005.

[27] C. Weber, T. Giamarchi, C. M. Varma, "Phase diagram of a three-orbital model for high-T_c cuprate superconductors", *Phys. Rev. Lett.* **112** (2014), article no. 117001.

[28] C. M. Varma, "Pseudogap and Fermi arcs in underdoped cuprates", *Phys. Rev. B* **99** (2019), article no. 224516.

[29] Y. Wang, A. Chubukov, "Charge-density-wave order with momentum (2Q,0) and (0,2Q) within the spin-fermion model: continuous and discrete symmetry breaking, preemptive composite order, and relation to pseudogap in hole-doped cuprates", *Phys. Rev. B* **90** (2014), article no. 035149.

[30] T. C. Hsu, J. B. Marston, I. Affleck, "Two observable features of the staggered-flux phase at nonzero doping", *Phys. Rev. B* **43** (1991), p. 2866-2877.

[31] S. Chakravarty, R. B. Laughlin, D. K. Morr, C. Nayak, "Hidden order in the cuprates", *Phys. Rev. B* **63** (2001), article no. 094503.

[32] A. Kaminski, S. Rosenkranz, H. M. Fretwell, J. Campuzano, Z. Li, H. Raffy, W. G. Cullen, H. You, C. G. Olson, C. M. Varma, H. Höchst, "Spontaneous breaking of time-reversal symmetry in the pseudogap state of a high-T_c superconductor", *Nature* **416** (2002), p. 610-613.

[33] V. Balédent, B. Fauqué, Y. Sidis, N. B. Christensen, S. Pailhès, K. Conder, E. Pomjakushina, J. Mesot, P. Bourges, "Two-dimensional orbital-like magnetic order in the high-temperature $La_{2-x}Sr_xCuO_4$ superconductor", *Phys. Rev. Lett.* **105** (2010), article no. 027004.

[34] S. De Almeida-Didry, Y. Sidis, V. Balédent, F. Giovannelli, I. Monot-Laffez, P. Bourges, "Evidence for intra-unit-cell magnetic order in $Bi_2Sr_2CaCu_2O_{8+\delta}$", *Phys. Rev. B* **86** (2012), article no. 020504.

[35] L. Mangin-Thro, Y. Sidis, P. Bourges, S. De Almeida-Didry, F. Giovannelli, I. Laffez-Monot, "Characterization of the intra-unit-cell magnetic order in $Bi_2Sr_2CaCu_2O_{8+\delta}$", *Phys. Rev. B* **89** (2014), article no. 094523.

[36] J. Jeong, Y. Sidis, A. Louat, V. Brouet, P. Bourges, "Time-reversal symmetry breaking hidden order in $Sr_2(Ir,Rh)O_4$", *Nat. Commun.* **8** (2017), article no. 15119.

[37] D. Bounoua, L. Mangin-Thro, J. Jeong, R. Saint-Martin, L. Pinsard-Gaudart, Y. Sidis, P. Bourges, "Loop currents in two-leg ladder cuprates", *Commun. Phys.* **3** (2020), no. 1, article no. 123.

[38] M. S. Scheurer, S. Sachdev, "Orbital currents in insulating and doped antiferromagnets", *Phys. Rev. B* **98** (2018), article no. 235126.

[39] D. F. Agterberg, D. S. Melchert, M. K. Kashyap, "Emergent loop current order from pair density wave superconductivity", *Phys. Rev. B* **91** (2015), article no. 054502.

[40] Z. Dai, Y.-H. Zhang, T. Senthil, P. A. Lee, "Pair-density waves, charge-density waves, and vortices in high-T_c cuprates", *Phys. Rev. B* **97** (2018), article no. 174511.

[41] S. Sarkar, D. Chakraborty, C. Pépin, "Incipient loop-current order in the underdoped cuprate superconductors", *Phys. Rev. B* **100** (2019), article no. 214519.

[42] Y. Sidis, B. Fauqué, V. Aji, P. Bourges, "Search for the existence of circulating currents in high-T_c superconductors using the polarized neutron scattering technique", *Phys. B: Condens. Matt.* **397** (2007), no. 1, p. 1-6.

[43] P. Bourges, Y. Sidis, "Novel magnetic order in the pseudogap state of high-T_c copper oxides superconductors", *C. R. Phys.* **12** (2011), no. 5, p. 461-479, Superconductivity of strongly correlated systems.

[44] Y. Sidis, P. Bourges, "Evidence for intra-unit-cell magnetic order in the pseudo-gap state of high-T_c cuprates", *J. Phys.: Conf. Ser.* **449** (2013), article no. 012012.

[45] P. Bourges, D. Bounoua, J. Jeong, L. Mangin-Thro, Y. Sidis, "Evidence for intra-unit cell magnetism in superconducting cuprates: a technical assessment", *J. Phys.: Conf. Ser.* **1316** (2019), article no. 012003.

[46] T. P. Croft, E. Blackburn, J. Kulda, R. Liang, D. A. Bonn, W. N. Hardy, S. M. Hayden, "No evidence for orbital loop currents in charge-ordered $YBa_2Cu_3O_{6+x}$ from polarized neutron diffraction", *Phys. Rev. B* **96** (2017), article no. 214504.

[47] P. Bourges, Y. Sidis, L. Mangin-Thro, "Comment on "No evidence for orbital loop currents in charge-ordered $YBa_2Cu_3O_{6+x}$ from polarized neutron diffraction"", *Phys. Rev. B* **98** (2018), article no. 016501.

[48] S. W. Lovesey, D. D. Khalyavin, U. Staub, "Ferro-type order of magneto-electric quadrupoles as an order-parameter for the pseudo-gap phase of a cuprate superconductor", *J. Phys.: Condens. Matt.* **27** (2015), no. 29, article no. 292201.

[49] S. W. Lovesey, D. D. Khalyavin, "Ordered state of magnetic charge in the pseudo-gap phase of a cuprate superconductor ($HgBa_2CuO_{4+\delta}$)", *J. Phys.: Condens. Matt.* **27** (2015), no. 49, article no. 495601.

[50] M. Fechner, M. J. A. Fierz, F. Thöle, U. Staub, N. A. Spaldin, "Quasistatic magnetoelectric multipoles as order parameter for pseudogap phase in cuprate superconductors", *Phys. Rev. B* **93** (2016), article no. 174419.

[51] B. Hennion, "La diffusion inélastique des neutrons sur monocristal. Le spectromètre 3-axes", *JDN* **10** (2010), p. 357-378.

[52] Y. Ishikawa, K. Tajima, D. Bloch, M. Roth, "Helical spin structure in manganese silicide MnSi", *Solid State Commun.* **19** (1976), no. 6, p. 525-528.

[53] M.-H. Julien, "Magnetic order and superconductivity in $La_{2-x}Sr_xCuO_4$: a review", *Phys. B: Condens. Matt.* **329–333** (2003), p. 693-696, Proceedings of the 23rd International Conference on Low Temperature Physics.

[54] P. Chudzinski, M. Gabay, T. Giamarchi, "Orbital current patterns in doped two-leg Cu–O Hubbard ladders", *Phys. Rev. B* **78** (2008), article no. 075124.

[55] J. Xia, E. Schemm, G. Deutscher, S. A. Kivelson, D. A. Bonn, W. N. Hardy, R. Liang, W. Siemons, G. Koster, M. M. Fejer, A. Kapitulnik, "Polar Kerr-effect measurements of the high-temperature $YBa_2Cu_3O_{6+x}$ superconductor: evidence for broken symmetry near the pseudogap temperature", *Phys. Rev. Lett.* **100** (2008), article no. 127002.

[56] R. Daou, J. Chang, D. LeBoeuf, O. Cyr-Choinière, F. Laliberté, N. Doiron-Leyraud, B. J. Ramshaw, R. Liang, D. A. Bonn, W. N. Hardy, L. Taillefer, "Broken rotational symmetry in the pseudogap phase of a high-T_c superconductor", *Nature* **463** (2010), p. 519-522.

[57] Y. Lubashevsky, L. Pan, T. Kirzhner, G. Koren, N. P. Armitage, "Optical birefringence and dichroism of cuprate superconductors in the THz regime", *Phys. Rev. Lett.* **112** (2014), article no. 147001.

[58] L. Zhao, C. A. Belvin, R. Liang, D. A. Bonn, W. N. Hardy, N. P. Armitage, D. Hsieh, "A global inversion-symmetry-broken phase inside the pseudogap region of $YBa_2Cu_3O_y$", *Nat. Phys.* **13** (2017), p. 250-254.

[59] H. Murayama, K. Ishida, R. Kurihara, T. Ono, Y. Sato, Y. Kasahara, H. Watanabe, Y. Yanase, G. Cao, Y. Mizukami, T. Shibauchi, Y. Matsuda, S. Kasahara, "Bond directional anapole order in a spin-orbit coupled Mott insulator $Sr_2(Ir_{1-x}Rh_x)O_4$", *Phys. Rev. X* **11** (2021), article no. 011021.

[60] S. Lim, C. M. Varma, H. Eisaki, A. Kapitulnik, "Observation of broken inversion and chiral symmetries in the pseudogap phase in single and double layer bismuth-based cuprates", https://arxiv.org/abs/2011.06755, 2020.

[61] A. Shekhter, C. M. Varma, "Considerations on the symmetry of loop order in cuprates", *Phys. Rev. B* **80** (2009), article no. 214501.

[62] S. Di Matteo, M. R. Norman, "Orbital currents, anapoles, and magnetic quadrupoles in CuO", *Phys. Rev. B* **85** (2012), article no. 235143.

[63] N. A. Spaldin, M. Fiebig, M. Mostovoy, "The toroidal moment in condensed-matter physics and its relation to the magnetoelectric effect", *J. Phys.: Condens. Matt.* **20** (2008), no. 43, article no. 434203.

[64] V. Aji, A. Shekhter, C. M. Varma, "Theory of the coupling of quantum-critical fluctuations to fermions and d-wave superconductivity in cuprates", *Phys. Rev. B* **81** (2010), article no. 064515.

[65] Y. He, C. M. Varma, "Theory of polarized neutron scattering in the loop-ordered phase of cuprates", *Phys. Rev. B* **86** (2012), article no. 035124.

[66] J. Orenstein, "Optical nonreciprocity in magnetic structures related to high-T_c superconductors", *Phys. Rev. Lett.* **107** (2011), article no. 067002.

[67] V. M. Yakovenko, "Tilted loop currents in cuprate superconductors", *Phys. B: Condens. Matt.* **460** (2015), p. 159-164, Special Issue on Electronic Crystals (ECRYS-2014).

[68] S. Lederer, S. A. Kivelson, "Observable NMR signal from circulating current order in YBCO", *Phys. Rev. B* **85** (2012), article no. 155130.

[69] S. Chatterjee, S. Sachdev, "Insulators and metals with topological order and discrete symmetry breaking", *Phys. Rev. B* **95** (2017), article no. 205133.

[70] M. J. Lawler, K. Fujita, J. Lee, A. R. Schmidt, Y. Kohsaka, C. K. Kim, H. Eisaki, S. Uchida, J. C. Davis, J. P. Sethna, E.-A. Kim, "Intra-unit-cell electronic nematicity of the high-T_c copper-oxide pseudogap states", *Nature* **466** (2010), p. 347-351.

[71] S. Mukhopadhyay, R. Sharma, C. K. Kim, S. D. Edkins, M. H. Hamidian, H. Eisaki, S.-i. Uchida, E.-A. Kim, M. J. Lawler, A. P. Mackenzie, J. C. S. Davis, K. Fujita, "Evidence for a vestigial nematic state in the cuprate pseudogap phase", *Proc. Natl Acad. Sci. USA* **116** (2019), no. 27, p. 13249-13254.

[72] N. Auvray, B. Loret, S. Benhabib, M. Cazayous, R. D. Zhong, J. Schneeloch, G. D. Gu, A. Forget, D. Colson, I. Paul, A. Sacuto, Y. Gallais, "Nematic fluctuations in the cuprate superconductor $Bi_2Sr_2CaCu_2O_{8+\delta}$", *Nat. Commun.* **10** (2019), article no. 5209.

[73] M. H. Fischer, E.-A. Kim, "Mean-field analysis of intra-unit-cell order in the Emery model of the CuO_2 plane", *Phys. Rev. B* **84** (2011), article no. 144502.

[74] A. Sacuto, S. Benhabib, Y. Gallais, S. Blanc, M. Cazayous, M.-A. Méasson, J. S. Wen, Z. J. Xu, G. D. Gu, "Pseudogap in cuprates by electronic Raman scattering", *J. Phys.: Conf. Ser.* **449** (2013), article no. 012011.

[75] I. M. Vishik, M. Hashimoto, R.-H. He, W.-S. Lee, F. Schmitt, D. Lu, R. G. Moore, C. Zhang, W. Meevasana, T. Sasagawa, S. Uchida, K. Fujita, S. Ishida, M. Ishikado, Y. Yoshida, H. Eisaki, Z. Hussain, T. P. Devereaux, Z.-X. Shen, "Phase competition in trisected superconducting dome", *Proc. Natl Acad. Sci. USA* **109** (2012), no. 45, p. 18332-18337.

[76] R. Dipasupil, M. Oda, N. Momono, M. Ido, "Energy gap evolution in the tunneling spectra of $Bi_2Sr_2CaCu_2O_{8+\delta}$", *J. Phys. Soc. Japan* **71** (2002), no. 6, p. 1535-1540.

[77] L. Ozyuzer, J. F. Zasadzinski, K. E. Gray, C. Kendziora, N. Miyakawa, "Absence of pseudogap in heavily overdoped $Bi_2Sr_2CaCu_2O_{8+\delta}$ from tunneling spectroscopy of break junctions", *Europhys. Lett.* **58** (2002), no. 4, p. 89-595.

[78] T. Watanabe, T. Fujii, A. Matsuda, "Anisotropic resistivities of precisely oxygen controlled single-crystal $Bi_2Sr_2CaCu_2O_{8+\delta}$: systematic study on "Spin Gap" effect", *Phys. Rev. Lett.* **79** (1997), p. 2113-2116.

[79] Y. Toda, F. Kawanokami, T. Kurosawa, M. Oda, I. Madan, T. Mertelj, V. V. Kabanov, D. Mihailovic, "Rotational symmetry breaking in $Bi_2Sr_2CaCu_2O_{8+\delta}$ probed by polarized femtosecond spectroscopy", *Phys. Rev. B* **90** (2014), article no. 094513.

[80] B. Loret, N. Auvray, G. D. Gu, A. Forget, D. Colson, M. Cazayous, Y. Gallais, I. Paul, M. Civelli, A. Sacuto, "Universal relationship between the energy scales of the pseudogap phase, the superconducting state, and the charge-density-wave order in copper oxide superconductors", *Phys. Rev. B* **101** (2020), article no. 214520.

[81] B. Leridon, P. Monod, D. Colson, A. Forget, "Thermodynamic signature of a phase transition in the pseudogap phase of $YBa_2Cu_3O_x$ high-T_C superconductor", *Europhys. Lett.* **87** (2009), no. 1, article no. 17011.

[82] C. Varma, L. Zhu, "Specific heat and sound velocity at the relevant competing phase of high-temperature superconductors", *Proc. Natl Acad. Sci. USA* **112** (2015), p. 6331-6335.

[83] M. S. Grønsleth, T. B. Nilssen, E. K. Dahl, E. B. Stiansen, C. M. Varma, A. Sudbø, "Thermodynamic properties near the onset of loop-current order in high-T_c superconducting cuprates", *Phys. Rev. B* **79** (2009), article no. 094506.

[84] D. LeBoeuf, S. Kramer, W. N. Hardy, R. Liang, D. A. Bonn, C. Proust, "Thermodynamic phase diagram of static charge order in underdoped $YBa_2Cu_3O_y$", *Nat. Phys.* **9** (2013), p. 79-83.

[85] H.-H. Kim, S. M. Souliou, M. E. Barber, E. Lefrançois, M. Minola, M. Tortora, R. Heid, N. Nandi, R. A. Borzi, G. Garbarino, A. Bosak, J. Porras, T. Loew, M. König, P. J. W. Moll, A. P. Mackenzie, B. Keimer, C. W. Hicks, M. Le Tacon, "Uniaxial pressure control of competing orders in a high-temperature superconductor", *Science* **362** (2018), no. 6418, p. 1040-1044.

[86] S. Blanco-Canosa, A. Frano, T. Loew, Y. Lu, J. Porras, G. Ghiringhelli, M. Minola, C. Mazzoli, L. Braicovich, E. Schierle, E. Weschke, M. Le Tacon, B. Keimer, "Momentum-dependent charge correlations in $YBa_2Cu_3O_{6+\delta}$ superconductors probed by resonant X-ray scattering: evidence for three competing phases", *Phys. Rev. Lett.* **110** (2013), article no. 187001.

[87] H. Alloul, P. Mendels, H. Casalta, J. F. Marucco, J. Arabski, "Correlations between magnetic and superconducting properties of Zn-substituted $YBa_2Cu_3O_{6+x}$", *Phys. Rev. Lett.* **67** (1991), p. 3140-3143.

[88] H. Alloul, J. Bobroff, M. Gabay, P. J. Hirschfeld, "Defects in correlated metals and superconductors", *Rev. Mod. Phys.* **81** (2009), p. 45-108.

[89] C. M. Varma, "Pseudogap in cuprates in the loop-current ordered state", *J. Phys.: Condens. Matt.* **26** (2014), no. 50, article no. 505701.

[90] V. S. de Carvalho, C. Pépin, H. Freire, "Coexistence of Θ_{II}-loop-current order with checkerboard d-wave CDW/PDW order in a hot-spot model for cuprate superconductors", *Phys. Rev. B* **93** (2016), article no. 115144.

[91] R.-G. Cai, L. Li, Y.-Q. Wang, J. Zaanen, "Intertwined order and holography: the case of parity breaking pair density waves", *Phys. Rev. Lett.* **119** (2017), article no. 181601.

[92] E. Fradkin, S. A. Kivelson, J. M. Tranquada, "Colloquium: theory of intertwined orders in high temperature superconductors", *Rev. Mod. Phys.* **87** (2015), p. 457-482.

[93] A. M. Mounce, S. Oh, J. A. Lee, W. P. Halperin, A. P. Reyes, P. L. Kuhns, M. K. Chan, C. Dorow, L. Ji, D. Xia, X. Zhao, M. Greven, "Absence of static loop-current magnetism at the apical oxygen site in $HgBa_2CuO_{4+\delta}$ from NMR", *Phys. Rev. Lett.* **111** (2013), article no. 187003.

[94] T. Wu, H. Mayaffre, S. KrÀÂd'mer, M. Horvatic, C. Berthier, W. Hardy, R. Liang, D. Bonn, M.-H. Julien, "Incipient charge order observed by NMR in the normal state of $YBa_2Cu_3O_y$", *Nat. Commun.* **6** (2015), article no. 6438.

[95] A. Pal, K. Akintola, M. Potma, M. Ishikado, H. Eisaki, W. N. Hardy, D. A. Bonn, R. Liang, J. E. Sonier, "Investigation of potential fluctuating intra-unit cell magnetic order in cuprates by μSR", *Phys. Rev. B* **94** (2016), article no. 134514.

[96] A. Pal, S. R. Dunsiger, K. Akintola, A. C. Y. Fang, A. Elhosary, M. Ishikado, H. Eisaki, J. E. Sonier, "Quasistatic internal magnetic field detected in the pseudogap phase of $Bi_{2+x}Sr_{2-x}CaCu_2O_{8+\delta}$ by muon spin relaxation", *Phys. Rev. B* **97** (2018), article no. 060502.

[97] S. Gheidi, K. Akintola, A. C. Y. Fang, S. Sundar, A. M. Côté, S. R. Dunsiger, G. D. Gu, J. E. Sonier, "Absence of μSR evidence for magnetic order in the pseudogap phase of $Bi_{2+x}r_{2-x}CaCu_2O_{8+\delta}$", *Phys. Rev. B* **101** (2020), article no. 184511.

[98] Z. H. Zhu, J. Zhang, Z. F. Ding, C. Tan, C. S. Chen, Q. Wu, Y. X. Yang, O. O. Bernal, P.-C. Ho, G. D. Morris, A. Koda, A. D. Hillier, S. P. Cottrell, P. J. Baker, P. K. Biswas, J. Qian, X. Yao, D. E. MacLaughlin, L. Shu, "Muon spin relaxation and fluctuating magnetism in the pseudogap phase of $YBa_2Cu_3O_y$", *Phys. Rev. B* **103** (2021), article no. 134426.

[99] C. Tan, Z. F. Ding, J. Zhang, Z. H. Zhu, O. O. Bernal, P. C. Ho, A. D. Hillier, A. Koda, H. Luetkens, G. D. Morris, D. E. MacLaughlin, L. Shu, "Slow magnetic fluctuations and critical slowing down in $Sr_2Ir_{1-x}Rh_xO_4$", *Phys. Rev. B* **101** (2020), article no. 195108.

[100] X. Lu, D. Sénéchal, "Loop currents in ladder cuprates: a dynamical mean field theory study", *Phys. Rev. B* **102** (2020), article no. 085135.

[101] R. Tazai, Y. Yamakawa, H. Kontani, "Emergence of charge loop current in the geometrically frustrated Hubbard model: a functional renormalization group study", *Phys. Rev. B* **103** (2021), article no. L161112.

[102] M. Mitrano, A. A. Husain, S. Vig, A. Kogar, M. S. Rak, S. I. Rubeck, J. Schmalian, B. Uchoa, J. Schneeloch, R. Zhong, G. D. Gu, P. Abbamonte, "Anomalous density fluctuations in a strange metal", *Proc. Natl Acad. Sci. USA* **115** (2018), no. 21, p. 5392-5396.

[103] D. V. Else, T. Senthil, "Strange metals as ersatz Fermi liquids", https://arxiv.org/abs/2010.10523, 2020.

[104] C. Morice, D. Chakraborty, X. Montiel, C. Pépin, "Pseudo-spin skyrmions in the phase diagram of cuprate superconductors", *J. Phys.: Condens. Matt.* **30** (2018), no. 29, article no. 295601.

[105] M. Fiebig, "Revival of the magnetoelectric effect", *J. Phys. D: Appl. Phys.* **38** (2005), no. 8, p. R123-R152.

[106] M. Klug, J. Kang, R. M. Fernandes, J. Schmalian, "Orbital loop currents in iron-based superconductors", *Phys. Rev. B* **97** (2018), article no. 155130.

[107] V. Scagnoli, U. Staub, Y. Bodenthin, R. A. de Souza, M. García-Fernández, M. Garganourakis, A. T. Boothroyd, D. Prabhakaran, S. W. Lovesey, "Observation of orbital currents in CuO", *Science* **332** (2011), no. 6030, p. 696-698.

[108] Y. Joly, S. P. Collins, S. Grenier, H. C. N. Tolentino, M. De Santis, "Birefringence and polarization rotation in resonant X-ray diffraction", *Phys. Rev. B* **86** (2012), article no. 220101.

[109] A. de la Torre, K. L. Seyler, L. Zhao, S. Di Matteo, M. S. Scheurer, B. Yu, L. Y, M. Greven, S. Sachdev, M. R. Norman, D. Hsieh, "Mirror symmetry breaking in a model insulating cuprate", *Nat. Phys.* **17** (2021), p. 777-781.

[110] M. Hücker, M. v. Zimmermann, G. D. Gu, Z. J. Xu, J. S. Wen, G. Xu, H. J. Kang, A. Zheludev, J. M. Tranquada, "Stripe order in superconducting $La_{2-x}Ba_xCuO_4$ ($0.095 \leq x \leq 0.155$)", *Phys. Rev. B* **83** (2011), article no. 104506.